CHAPTER

Past and future hydrological drought

11

Niko Wanders[1], Christel Prudhomme[2,4,6], Jean-Philippe Vidal[3], Katie Facer-Childs[4] and James H. Stagge[5]

[1]*Physical Geography, Utrecht University, Utrecht, the Netherlands;* [2]*Forecast Department, European Centre for Medium-Range Weather Forecasts (ECMWF), Reading, United Kingdom;* [3]*RiverLy, INRAE, Villeurbanne, France;* [4]*UK Centre for Ecology & Hydrology (UKCEH), Wallingford, Oxfordshire, United Kingdom;* [5]*Department of Civil, Environmental and Geodetic Engineering, The Ohio State University, Columbus, OH, United States;* [6]*Geography Department, Loughborough University, Loughborough, United Kingdom*

Chapter outline

Hydrological Drought. https://doi.org/10.1016/B978-0-12-819082-1.00015-1

11.1 Introduction

While droughts repeatedly happen around the world, it is important to put these droughts into a historic perspective to understand their severity and impact. Not only are we interested in what has happened in the past, but also what is going to happen during future drought events, due to global change, that is, climate change and other human interventions. In this chapter, we take a closer look at these long-term trends taking a historic and future perspective on drought with a focus on three important periods: (a) the distant past, (b) the instrumental period, and (c) the future. These periods all have their own challenges and opportunities related to data availability and methods that can be used to quantify low flow and hydrological drought.

If you fully want to understand the impact of drought (Chapter 12), it is important to understand the historic and future climate variability and how this variability has protruded onto hydrological drought. This allows you to put projected future trends into a historical perspective and see if ongoing drought events are parts of a longer decadal or centennial trend. A good understanding of observed trends allows for a deeper understanding and better insights into the changes ahead.

Analysing droughts in the distant past, which roughly goes back to the 15th century (Section 11.2), helps to better understand long-term climate variability at different spatial scales, for example, for a given region or catchment. It will allow you to see if extreme droughts are part of the natural variability or whether a new climate signal emerges.

The instrumental period (Section 11.3) provides valuable and long-term information based on time series of measured hydrometeorological data needed for a broad set of drought characteristics (Chapter 5). In the instrumental period going back roughly to early 1800s, observations become more frequent and at a higher spatial density compared to the distant past, and in addition, new types of data become available, such as satellite observations. This allows for a more robust trend detection of hydrometeorological variables as well as low flow and drought indices derived thereof, covering more regions around the world and with global coverage towards the end of the period. Although records may not be as long as for the distant past, we do observe the first signals of climate change in this period.

Assessment of the future (Section 11.4) is vital to evaluate potential changes in drought characteristics as a result of climate change or more broadly global change. Notable changes already observed in greenhouse gas emissions have led to shifts in the hydrological cycle, also changing the frequency and severity of droughts around the world (Caretta et al., 2022). For obvious reasons, we have no observations of future droughts. This makes it difficult to give any exact estimates of future drought events, but a number of climate and hydrological model projections (simulated time series of hydroclimatic data) exist that provide valuable input for future analysis. Climate model projections

provide such information on future climate dynamics, but do not make any exact prediction on the occurrence of drought for a certain year in the future. Accordingly, when analysing the effect of climate change on a given hydroclimatic variable or drought characteristic, the focus is on changes and trends in statistics, such as mean and extreme values, over longer periods. The projected changes and trends in future drought characteristics can serve to inform policy and management decisions, implement adaptation strategies and improve general drought preparedness today and in the future.

By combing the information from these three periods, we can create a broad overview of changes and trends in drought characteristics across time. This information is key when considering changes in drought adaptation and policy, as it allows us to put future changes into a historic perspective. However, the challenges in obtaining representative time series differ considerably among the periods, and combining these adds to these challenges. One obvious challenge is the lack or complete absence of observations. For example, when looking at droughts before the start of the instrumental period, river flow records are not available and proxy data (e.g., tree rings) have to be deployed to estimate river flow. A proxy indicator is a local record that is interpreted using physical or biophysical principles to represent some combination of climate- or hydrology-related variations back in time. For the instrumental period, observations may be available, however, it is often difficult to get consistent long-term records, due to missing data, changes in measurement techniques or the effect of human interventions on hydrological variables (Chapter 10). Future droughts are subject to uncertainties in simulated time series from hydroclimate modelling.

In this chapter, we discuss how you can use different techniques to obtain historic drought records for the distant past. We discuss data availability and introduce different methods to reconstruct time series and associated droughts. For the instrumental period, we look at how we can obtain reliable drought records, how to use these time series for potential applications, such as investigation of major droughts and trend analysis (Section 11.3). In addition, we look at some specific aspects of data availability in the instrumental period not dealt with in Chapter 4. Finally, we will show how you can use projections, robust methods and workflows to project future drought (Section 11.4). We also briefly cover the influence of human interventions on future droughts building on Chapter 10. After reading this chapter, you should have gained knowledge on how to put current drought events into both a historic and future perspective, as well as understand the limitations and challenges that you will face when working on droughts in the distant past, instrumental period and future.

11.2 Distant past

11.2.1 Data availability

Proxy-based reconstructions use either natural or historic records of climate as stand-ins, or 'proxies', to make plausible estimates of the distant past climate or hydrology prior to the instrumental record (here back to the 15th century). Natural proxies can include physical or chemical measurements from tree rings, ice cores, sediment layers, corals and speleothems (growths of structures in caves), among others. Historic proxies can be contemporary historical records, such as written weather reports, qualitative or non-traditional gauges, reports of specific historical events or economic records, such as agricultural production (e.g., grape harvest, Možný et al., 2016).

Various types of proxy records can be useful for different climates and periods of interest. For example, ice cores take a long time to accumulate and only cover glacial regions, but do provide very

long records. Corals, on the other hand, are typically found in warmer oceans, but cover a shorter period in time. Therefore, it is important to select appropriate proxy methods according to your research question, region of interest and data available. A limitation of several drought proxy methods (e.g., ice cores, corals, lake sediments) is that they only allow you to reconstruct the climate signal (i.e., precipitation and temperature) and are less suited to reconstruct hydrological time series directly. This can be overcome by adding auxiliary information or combining proxy records, allowing you to look at different aspects of the hydrological cycle. For example, by combining sediment records with information from ice cores; sediment records provide information on annual average river flow, whereas ice cores provide information on average annual precipitation and regional temperatures.

Among natural proxies, tree-ring width has proven particularly effective for hydrologic reconstructions because for certain species and climates, tree growth in each year is limited by available water or energy, producing an annual chronology. Another benefit of tree-ring proxies is their combination of long records (multi-century) with an annual temporal resolution. In the following, we therefore focus on tree rings, as an example of a natural proxy reconstruction. However, the same general methodology is valid for other natural proxies, and many of the historical proxies that depend on statistical relationships with river flow.

11.2.2 Methods to reconstruct time series

Flow reconstructions using tree-rings first establish a statistical relationship between the proxy and observed river flow during the instrumental period and then assume this relationship to hold over time (Loaiciga et al., 1993). This allows for plausible estimates of annual or seasonal (summer and winter) flow for as long as proxy records are available. Usually, the interpretation of a proxy record is complicated by the presence of noise distorting the underlying information. Careful calibration and cross-validation procedures are necessary to establish a reliable relationship between a proxy indicator and the climatic or hydrological variable(s), providing a transfer function through which past hydroclimatic conditions can be estimated.

One may assume that trees growing along a riverbank would provide the best record of river flow, similar to a flow gauge; however, these riparian trees are generally not sensitive to variations in river flow because the soil is wet, or nearly saturated, even during drought, that is, the trees do not suffer from water limitations. Instead, trees that are highly sensitive to available water and energy in the region (in the case of high elevation sites) should be selected as representative sites. It is common to reconstruct drought years from the width or the density of annual growth rings.

For any proxy-based reconstruction, it is critical to have an understanding of the nature of the underlying proxy because a reconstruction is an extrapolation, that is, there are no gauge observations in the distant past to check your work. Each proxy has unique benefits and challenges, so it is preferable to engage with proxy experts. In the case of tree-rings, a single chronology is derived from ring width measurements of 10 or more trees of the same species at a single site. Typically, 30–60 cores are taken at a site with preferably more than one core per tree. To create a tree-ring chronology, cores from the sampled trees at each site are cross dated (that is, patterns of narrow and wide rings are matched from tree to tree) to account for missing or false rings, so that every annual ring is dated to the correct year. Growth-related trends (that is, unrelated to climate, such as tree age) must then be statistically removed before the ring width values for each year are averaged to create a time series of annual ring-width indices, called the tree-ring chronology. Understanding this process and the

peculiarities of the particular species is critical to avoid producing models that fit well, but may not have a realistic basis.

11.2.3 Drought in the distant past

Some severe droughts have occurred in the distant past, leading to the collapse of civilisations and causing catastrophic damage. For example, the collapse of the Maya civilisation is linked to extreme drought events between 800 and 1000 CE. Evans et al. (2018) used lake sediment records to reconstruct drought during this period by looking at the isotopic composition of ancient lake water in gypsum in the lake sediments. Based on the composition, they were able to detect historic drought periods in the sedimentary record. They then used a statistical model to reconstruct the annual precipitation time series. Although the method provides a nice overview of the influence of drought on the lake depth, it is difficult – as for all physical proxies – to estimate whether it was a long dry period or several short intense droughts.

Neukom et al. (2010a) showed that qualitative sources (i.e., historic archives) can also be helpful, for example, newspaper records, when used in combination with tree rings, lake sediments, marine sediments, ice cores or corals. Using a Principal Component Regression (Box 8.3) for the instrumental period, they established a relationship between proxy records and statistically simulated climate data. Assuming the relationships to be stable in time, a meteorological reconstruction over South America was made, where the proxy records from the distant past were used to constrain the model simulations. This dataset now provides estimates of annual air temperature for southern South America beginning in the 900s CE. In Neukom et al. (2010b), the authors added a reconstructed annual precipitation dataset that goes back to 1500 CE. The datasets are both constrained on a small number of proxy observations as records that go that far back are limited. Despite being restricted to inter-annual variability, these types of datasets provide valuable consistent, observation-constrained records that can be very useful for drought analysis over longer time periods.

Tree-ring proxies used to reconstruct river flow on most continents are receiving expanded interest in water resilience planning (Meko et al., 2001; Woodhouse et al., 2006; Tingstand et al., 2014). For example, reconstructions extending the Colorado River in the United States by over 1200 years have been used to simulate the risk of joint occurrence of increasing water demands and the re-occurrence of historical droughts with millennium-length return periods (Woodhouse et al., 2010). Tree-ring reconstruction was also used to place the 2012–14 California drought and the 1930s 'Dust Bowl' drought into historic context, showing that each event was the worst of the last millennium for their locations, but were not considered outliers to be ignored in drought planning (Griffin and Anchukaitis, 2014; Cook et al., 2015). Flow reconstruction also blends hydrologic process understanding with proxy reconstruction to generate more physically realistic reconstructions and explore sub-annual resolutions (Sauchyn and Ilich, 2017; Stagge et al., 2018).

11.2.3.1 Reconstruction of summer drought in the Potomac River using tree rings

To illustrate the process of tree-ring drought reconstruction, we take a more detailed look at the work from Torbenson and Stagge (2021). In this study, the authors make a historical reconstruction of 350 years of river flow data for the Potomac River (at Point of Rocks, Maryland) using tree-ring chronologies. The methodology is presented below, along with a general guideline to river flow reconstruction from tree-ring chronologies.

Firstly, the authors filter for tree-ring chronologies that appear to have a connection with the climate variable of interest, in this case summer or winter base flow. This filtering is done based on linear correlation (Section 7.3.2) and an understanding of tree physiology to ensure the link makes physical sense. Following this, multiple chronologies with a strong connection are combined into a single tree-ring record using Principal Component Analyses (PCA, Section 7.5.3). Next, a model for river flow is calibrated using linear regression (Section 7.3.1) during the period common to tree-rings and observed flow (1931−80). This creates an equation or reconstruction model that fits a statistical relationship between the observed summer hydrology and thus summer droughts and the tree-ring data.

This model is then subjected to validation tests to confirm that the model is not over-fit or too sensitive to the specific data used to calibrate it. In this study, a holdout sample with observations from 1895−1929 was used for split-sample validation (Section 7.3.6). The linear regression (tree-ring width chronology and base flow) was fit from 1931−80 and then used to make predictions during the holdout period. Tree-ring growth proved to have a stronger relationship with base flow than with river flow for both summer and winter. Split-sample validation can be sampled to the breakpoint. In this case, the breakpoint was very near in time to some of the most severe droughts in the United States that occurred during the 1930s, so the authors chose to vary the split-sample to make sure the linear regression was stable. An alternative validation method is cross-validation or 'leave-one-out' procedure (Section 7.3.6). For example, the authors could have chosen to calibrate the linear relationship between tree-ring width and flow using 90% of the years and validate using the remaining 10%. Then, they would choose a different 90% for calibration and 10% for validation repeatedly until all years were considered for validation at least once.

Wherever possible, proxy-based reconstructions should be validated against historical documents or otherwise independent records. In this example, the authors found several historical reports of flood and drought in the pre-instrumental period that corroborated the reconstruction. Neukom et al. (2010a, 2010b) go into further detail regarding the use of historical records of the distant past in a study from South America.

Once convinced that the model is well calibrated (Fig. 11.1a) based on typical goodness-of-fit criteria (Section 7.3.4) and that the relationship is valid for the validation period, the model can be used to predict flows back in time for as long as the relevant proxies exist (Fig. 11.1b). In this example, the tree-ring chronologies included in the reconstruction model were available back to 1750. As you move further back in time, there are often fewer and fewer available chronologies. In the case of Torbenson and Stagge (2021), they were able to extend the reconstruction back to the year 1666 using models with progressively fewer predictors, shown as Nest 2 and 3 in Fig. 11.1b. With fewer chronologies, uncertainty tends to increase and calibration and validation statistics decrease until the reconstruction becomes uninformative. This is why this particular reconstruction ends in 1666 despite some chronologies extending further back in time.

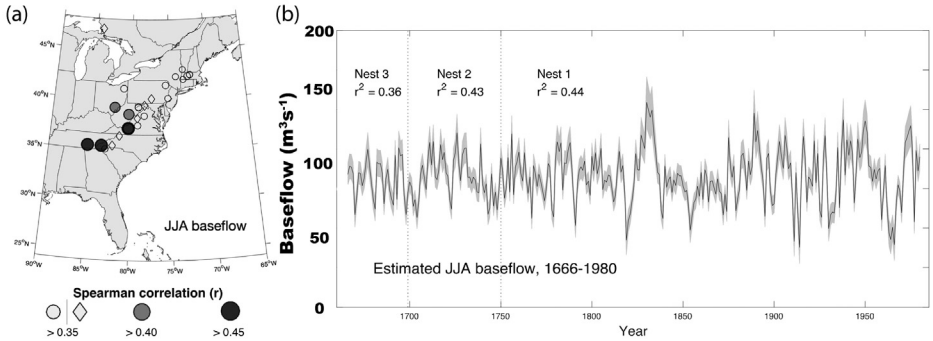

FIGURE 11.1

Reconstruction of June through August (JJA) base flow for the Potomac river (1666–1980): (a) chronologies included in reconstruction from tree-ring data are shown as symbols on the map, highlighting their correlation. *Circles* represent predictors from the current year and diamonds represent predictors from the following year (JJA only), and (b) the full area-average reconstruction time series of base flow is presented with 95% confidence *intervals shaded grey*. The different temporal evaluation periods (or Nests), and their statistics account for decreasing data availability in time. Nest 1 goes from 1750 to 1980, and the other Nests range from 1700–1980 (Nest 2) and 1650–1980 (Nest 3).

Modified from Torbenson et al. (2021).

11.2.3.2 Common approach using proxy records

The above example provides a common approach for drought reconstruction in the distant past using tree-ring chronologies. However, these general steps also apply to most cases where you need to reconstruct drought in the distant past based on other proxy records. When you follow these steps carefully, you will be able to reconstruct drought in the distant past based on a set of tree-ring chronologies or other proxy records and have an indication of their validity compared to independent observational data. Garnier (2019) provides a comprehensive overview of drought beyond the instrumental record in the United Kingdom, France and Germany building upon historical information derived from different archives (e.g., church, military, private diaries). He introduced the Historical Severity Drought Scale (HSDS), which helps to translate qualitative information into an index that varies from 1 (no drought) to 5 (exceptional drought). The HSDS is meant to describe the chronological variation and severity of droughts and in particular, the major droughts in the UK, Ile-de-France (Paris and surrounding) and the Upper Rhine Valley since around 1500. Anchukaitis (2017) gives a more detailed discussion of the nuances of proxy-based reconstruction.

11.3 Instrumental period

11.3.1 Observed time series of hydrometeorological data

While the distant past (Section 11.2) provides a series of challenges with regard to data collection and processing, the data availability in the instrumental period is significantly better (Chapter 4). Droughts in the instrumental period can be studied using data from a multitude of sources. Observed time series of hydrometeorological variables, such as precipitation, temperature, soil moisture, river flow and

groundwater (Sections 4.3–4.4) can all provide fundamental information for assessments of low flow and hydrological drought (first approach). They play a key role in benchmarking natural drought variability, exploring possible trends and improving preparedness for future drought. Hence, society encourages data rescue, restoration and modelling to extend current record lengths for the instrumental period.

The earliest records of hydrological variables go back to the ancient Chinese, Mesopotamian and Egyptian civilisations, for example, Egyptian officials have gauged the water levels of the Nile River for more than 5000 years (URL 11.1). In Europe, more permanent records of meteorological and hydrological variables dates back to about the early 1800s. However, data coverage is overall sparse before the mid-20th century (Section 4.3). This means that identifying drought earlier is only possible for individual catchments or smaller regions and will be challenging on a national, continental or global scale (Ionita et al., 2021). For these large scales, you will have to rely on modelling to bridge the gap between sparse observational records and data needed for large-scale analysis (Section 4.4 and Ionita et al., 2021).

The reliability of the identified hydrological drought characteristics in the instrumental period highly depends on the type and quality of the available data. Having multiple observed hydrometeorological variables can help you to look for consistency among these variables. However, it will not always be a feasible option, especially when you want to look at periods before 1950. In general, meteorological variables, such as temperature and precipitation, are often more readily available than river flow data and in particular, long-term groundwater data, which usually are very sparse. Temperature and precipitation records are commonly used to derive meteorological drought indices (Box 5.3), but also provide valuable input for drought identification using hydrological modelling reconstructions (Section 11.3.2). The meteorological information can come from observations (Section 4.4) or from global meteorological reanalysis datasets, which combine outputs from a global numerical weather prediction model and ground-based observations – as well as space-born observations in some datasets (Section 9.2).

You can also take advantage of simulated river flow and groundwater variables to overcome existing data gaps in the observations (Section 4.3.7.4). The advantage and disadvantages of the different data sources are discussed in detailed in Boxes 9.4 and 10.1.

11.3.2 Generation of hydrological time series

When sufficiently long time series of observed hydrological data (commonly $\geqslant$30 years) are lacking or the time series contains significant gaps, several methods can be applied to infill and extend the time series. One option is the use of stochastic simulation, which allows the generation of longer time series with similar statistical characteristics as the observed series (Section 7.2; Brunner et al., 2020). Long time series of river flow and groundwater can also be generated using a process-based hydrological model (Sections 9.3 and 9.4), given that the necessary meteorological forcing data are available, either as observations (first approach, Section 11.3.1), data rescue (second approach, Section 11.3.2.1) or reanalysis datasets (third approach, Section 11.3.2.2). The use of hydrological models allows for different forcing datasets and model parameters to be used, creating an ensemble of hydrological simulations and thus, implicitly an assessment of model uncertainties. The number and variety of process-based hydrological modelling studies to identify droughts are numerous (Sections 9.3 and 9.4); in this chapter, we focus on large-scale studies, from the national to the global scale.

In the instrumental period, hydrological models can be forced by time series of observed meteorological data (first approach, Section 11.3.1). However, in case of sparse observations, including time series with gaps or of insufficient length, which particularly applies to the instrumental period prior to 1950, we have to reconstruct time series of meteorological variables requested as input to the

hydrological models. As mentioned in Sections 4.3.8, 11.3.1 and 11.3.3, data rescue of documentary records can be used to reconstruct or recover time series of meteorological data (second approach, Section 11.3.2.1). While methodologies for drought data rescue (digitising analogue observations) are highly dependent on the type of documentary source (Sections 4.3.8 and 11.3.1), most methods to reconstruct time series rely on a symbiosis of models and observations where the latter are used to constrain the model simulations. Generation of time series of historical meteorological data (forcings) is done both for local, catchment scale studies as well as for large-scale modelling studies using interpolated observed data or gridded forcing from climate models (third approach, Section 11.3.2.2). Gridded time series of historical meteorological data are specifically used as input to large-scale models, that is, global hydrological models (GHMs) or land surface models (LSMs), to generate spatially distributed (i.e., gridded) time series of hydrological variables (Section 9.2). Subsequently, simulated time series of hydrological variables can be used to derive spatial drought characteristics (Section 5.7). Below two of the three approaches to generate time series of hydrological data are described, namely, the use of: (a) extended time series of meteorological data through data rescue, and (b) gridded time series of meteorological data. The first approach, which uses observed meteorological data (Section 11.3.1) to simulate time series of hydrological data, is rather straightforward (Section 9.3.3), and examples of its applications are described in Section 11.3.3.

11.3.2.1 Generation of river flow series using hydrological models forced by extended time series of meteorological data

In the period prior to 1950, time series of meteorological and hydrological data are scarce, and hence, efforts have been made to extend these. Smith et al. (2019) simulated time series of river flow in the United Kingdom since 1891 by using recovered weather records as forcing to water balance models (second approach). As part of a data rescue activity, over 200 monthly and 38 daily rain records for the period before 1910 were added. The observations were spatially interpolated using an inverse distance approach to generate time series of precipitation. Potential evapotranspiration (Section 3.3.1.1) was obtained from a gridded temperature dataset (Tanguy et al., 2018). These derived gridded datasets were then used as forcings to simulate daily river flow for 303 catchments across the United Kingdom, that is, to reconstruct river flow at a national scale back to 1891. The reconstructed time series allowed to obtain hydrological drought characteristics and put recent droughts in a broader historic perspective (Barker et al., 2019). Further details of the study are discussed in Section 11.3.3 below.

A similar approach was followed by Caillouet et al. (2017), which reconstructed low flow in France since 1871 by forcing a hydrologic model with, in this case, downscaled meteorological data (Box 11.1). The meteorological data were statistically downscaled from the 20th century global reanalysis (Compo et al., 2011) for the period 1871−2012 through an analogue resampling method building on a multi-variable surface reanalysis available over the past few decades only (Caillouet et al., 2019). As an advantage, the authors could use the more advanced Penman-Monteith potential evapotranspiration approach (Section 3.3.1.1), which is less sensitive to temperature trends. Caillouet et al. (2021) in a follow-up study refined their century-long assessment of spatio-temporal low flow events in France by taking advantage of a 142-year long meteorological reanalysis dataset (Devers et al., 2021) and an innovative hydrological reanalysis dataset combining river flow simulations and observations, together with their respective uncertainties.

The low flow and drought quantification methods outlined in Sections 5.3−5.7 require time series of sufficient length (varying from years to decades) to establish a benchmark and to quantify deviations from the benchmark. The same methods can be applied to simulated (or modelled)

hydrometeorological records. The advantage of the longer records for most indices is that it provides a more robust drought estimate and is also better suited to study trends and changes in drought indices (Section 7.4). Such trends and changes provide valuable information for assessments of future drought and in the analysis of causalities between drought and its drivers (Section 11.4).

11.3.2.2 Generation of river flow series using large-scale hydrological models and gridded meteorological data

Large-scale models, that is, GHMs and LSMs (Section 9.4.2) applied for continental and global scale drought studies (third approach) need information on the drivers of the hydrological system, typically precipitation and potential evapotranspiration (Fig. 11.2). Only in an ideal world, would a nearby meteorological station be available at each grid point and some kind of interpolation would always be required to obtain a grid (average) representative value (or for separate tiles within a grid cell). Datasets based on interpolated observations are commonly referred to as 'gridded observed'. In response to having no nearby meteorological station, several categories of large-scale gridded weather datasets have been developed, which combine climate models with meteorological observations (Fig. 9.2). These datasets are commonly called 'simulated observed' (sometimes 'proxy observed') to distinguish from gridded estimated observed (Section 9.2).

The instrumental period is covered by several such gridded datasets, referred to as gridded observed or simulated observed. While providing unique opportunities for drought analysis, such generated datasets also bring challenges that we have to address. Generated meteorological datasets generally have a global coverage and a high temporal resolution (daily or finer). Generation of temperature and precipitation is commonly done at spatial resolutions $<$50 km, with the current standard ERA5 land providing 10 km spatial resolution at the global scale. Some large-scale hydrological models, for example, LISFLOOD (Burek et al., 2013, Table 9.2), simulate runoff (mm day^{-1}) and river flow (m^3 s^{-1}) at a denser spatial scale (5 km), which calls for downscaling and bias correction of the climate model output (Box 11.1). Various bias correction methods have been developed to post-process model outputs to match observations. Downscaling and bias correction are also essential to infer the evolution of historic hydrological drought in small ungauged catchments, especially when located in areas with high elevation gradients that are not resolved at a large spatial scale.

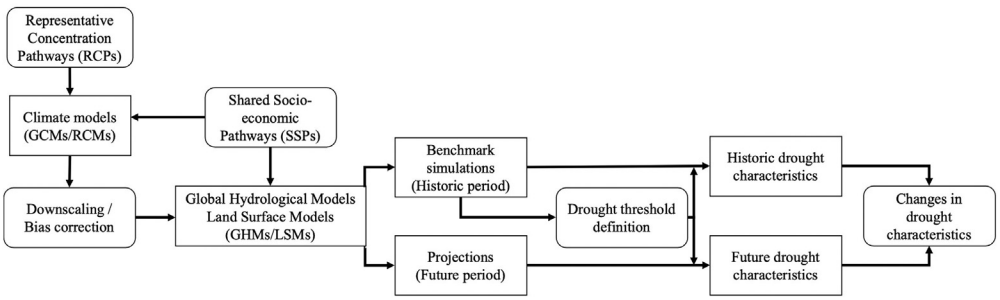

FIGURE 11.2

Example workflow for making drought projections (based on the threshold level approach, Section 5.4.1) using one or an ensemble of hydrological models.

Box 11.1 Downscaling and bias correction

When using data from large-scale climate models, you have to account for the variations that occur at spatial resolutions smaller than the Global Climate Model. To take these smaller scale variations into account, some form of downscaling and/or bias correction is needed. Here, we describe a workflow that could help you decide what is best for your specific task. Such a workflow is highly recommended when working with climate projections, but can also be useful when working with large-scale information for the instrumental period, for example, to define benchmark drought conditions.

Downscaling climate data can be done in two ways: (a) Dynamical Downscaling Methods (DDM), or (b) Statistical Downscaling Methods (SDM). Dynamical downscaling involves Regional Climate Models (RCMs), which use information from the Global Climate Models (GCMs) as boundary conditions to resolve the meteorology at finer scales, going down to 5−10 km. For smaller domains, even finer spatial resolutions can be used. The GCM projections are used as lateral meteorological boundary conditions. The RCM is not only applied for projections, but can also be used to make finer atmospheric simulations to simulate historic records of meteorological data. This can be especially useful when dealing with complex topographic terrain or events that produce extreme severe weather (such as severe thunderstorms).

Statistical downscaling involves calibrating a statistical relationship between large-scale information from global reanalyses, GCMs, or from RCMs, and local meteorological variables. Numerous SDMs have been developed over the last decades. They have different levels of complexity and can correct for the following aspects:

(a) biases in the data
(b) 'drizzle' days in large scale precipitation simulations
(c) deviations from the observational seasonality
(d) geographical inconsistencies.

The more meteorological variables that need to be corrected, the more difficult the statistical downscaling will be. The 'drizzle' days are a common problem in GCM and RCM simulations, where they provide rain on too many days as a result of the spatial resolution. When studying drought, it is especially important to look at these artefacts and whenever possible correct for their presence. The frequent drizzle may terminate the development of drought events in the models that we know have occurred from historic observations.

Simple bias correction methods look at the first-order statistics to correct for errors in mean and standard deviation. However, more advanced bias-correction methods exist, where also the second and third-order statistics are taken into account. In addition, some methods also preserve geostatistical properties. You will find that when applying more complex methods, it becomes increasingly important to assume that the biases in the model are consistent, and thus systematic, in both the compared (historic) period and the simulation period (often the future). This means that the errors that the model makes in the historic period are similar to those that will be made in the future simulations and thus similar corrections can be applied. More details regarding SDM techniques are provided in Forzieri et al. (2014) and Pan et al. (2021).

A recommended workflow (Fig. 11.3) for deriving smaller scale meteorological time series from GCM or RCM data may be articulated as:

(a) select a downscaling method, which can be dynamical (DDM in combination with a RCM) or statistical (SDM)
(b) if an SDM has been selected, it has to be calibrated and validated against local observations (e.g., Cucchi et al., 2020)
(c) apply the downscaling method (either DDM in combination with a RCM or SDM) to the GCM output (in case of downscaling global climate model output). At the continental scale, the RCM output can be downscaled to more detailed scales (e.g., regions, nations) in the same way
(d) assess the downscaling uncertainty: (a) reiterate with different SDMs or RCMs, and/or (b) reiterate with alternative large-scale forcing datasets (e.g., alternative reanalysis datasets).

The above workflow can be applied, for example, to obtain meteorological time series at the continental scale derived from global climate output (Fig. 11.3, middle and upper row) or to obtain time series at the catchment scale derived from continental scale climate output (Fig. 11.3, middle and lower row). The workflow, which applies to GCM and RCM outcome, can also be used to downscale and bias correct large-scale reanalysis data (Caillouet et al., 2019). For further reading, we refer to Maraun et al. (2015) and Maraun and Widmann (2018).

Continued

Box 11.1 Downscaling and bias correction—cont'd

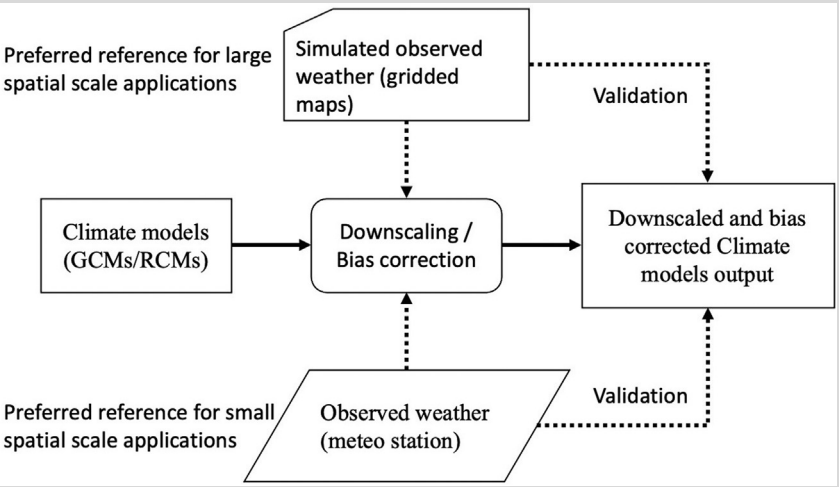

FIGURE 11.3

Example workflow for downscaling of climate model output. At large spatial scales the bias correction can be done using gridded maps, whereas for small-scale applications local meteorological station data can be used to correct for biases in the climate model simulations.

11.3.3 Drought in the instrumental period

This section presents droughts in the instrumental period using different types of historical data: (a) simulated time series of hydrological variables using observed meteorological data (first approach, Section 11.3.1), (b) simulated time series of hydrological data using reconstructed or recovered meteorological data (second approach, Section 11.3.2), and (c) simulated time series of hydrological data obtained with large-scale hydrological models and gridded meteorological data (third approach, Section 11.3.2).

11.3.3.1 Drought derived from observed time series of hydrometeorological data

Droughts derived from time series of observed hydrometeorological data (first approach, Section 11.3.1) have the obvious advantage that no reconstruction or modelling uncertainties entail, which makes these series suitable as a benchmark. However, observational uncertainties must still be considered as these may be high for the lowest flows (Section 4.2.6). Studies based on observed data serve several purposes, among other the identification of the causes of specific droughts, their drivers (Chapter 2), how hydrological processes are affected (Chapter 3), how these processes influence drought characteristics (Chapter 5) and impacts (Chapter 12). Here, we present a number of studies that describe historical hydrological drought. The first set of studies are about trends in hydrological drought, starting with a global scale study followed by trend investigations at the continental scale (Europe) and national scale (USA). This is followed by a series of studies describing two major large-scale droughts in Europe, that is, the 2015 drought in central Europe and the 2018 drought in northern Europe.

Several large-scale studies investigate regional and continental scale trends in annual or seasonal river flow, differing among other in the choice of drought indices, period analysed and spatial resolution. Fewer studies address the global scale, and there is currently low confidence in the sign and magnitude of river flow trends at the global scale, even more so for low flow and hydrological drought. Gudmundsson et al. (2019) assessed trends in low and high flow as well as in the mean flow, using daily observed river flow from a global dataset. Trends were analysed for three overlapping 40-year periods (1951−2010). Low flow indices included time series of annual minimum, $AM(1\text{-day})$, flow and the Q_{90} (Box 5.1). The authors found that in most regions, the sign of regional trends was consistent across indices, that is, increasing low flow was associated with increasing mean and high flows. The strongest trend towards drier conditions was found for southern Europe and the Mediterranean. The number of stations varied significantly among regions, with fewer data available in Asia and Africa, and the spatiotemporal coverage limited the conclusions that could be made. It should be noted that no attempt was made to separate between the cause of the trends, that is, whether they were due to climate or human interventions.

Stahl et al. (2010) investigated trends in observed time series of low flow ($AM(7\text{-day})$) in more than 400 near-natural catchments from 15 countries across Europe covering the period 1962−2004. Overall, low flow wass found to decrease in regions with a summer low flow regime, whereas a mixed pattern was seen for catchments with winter minima (secondary minima in summer). Interestingly, looking at trends in monthly mean flow, a trend towards drier conditions was seen in almost all catchments in August. Hannaford et al. (2013) used a subset of these catchments (around 130) with flow records covering a longer period (1932−2004) to perform a multi-temporal trend analysis. They found that the magnitude and even direction of short-term trends were heavily influenced by inter-decadal variability. Some short-term trends uncovered in previous studies were shown not to be representative of long-term change. Accordingly, the long-term variability may serve as a reference for previous and future studies. It is concluded that future work should "attempt to explain the decadal-scale variations that drive short-term trends, and thus develop more sophisticated methods for trend detection that take account of interdecadal variability and its drivers". Spatial and temporal variability in flow intermittence over the period 1970−2018 across large regions (Australia, France, the United Kingdom and the conterminous USA) was analysed by Sauquet et al. (2021). Trends in the annual frequency of no flows (i.e., days with zero flow, Section 5.4.2) were derived for 1356 gauging stations in unregulated rivers. It was found that some, but not all, regions in Australia and the United States displayed significant trends in the occurrence of no-flow days, and if so, mostly an upward trend was detected.

Further zooming in on Europe, the central European drought of 2015 was systematically analysed by Ionita et al. (2017) and Laaha et al. (2017) in terms of drivers and spatial and temporal low flow patterns, respectively. Daily discharge observations from approximately 800 near-natural catchments across Europe were collected by an international team of researchers. A constant threshold (Q_{80}) (Box 5.1) was chosen to identify drought events in the time series. The period 1976−2010 was selected as a benchmark against which the drought characteristics of the year 2015 were compared. In addition, the characteristics of the 2015 event were compared to the year 2003, which affected almost the same region. The 2015 drought was caused by anomalies in the pressure systems and anomalously warm sea surface temperatures in the Mediterranean. This resulted in strong discharge anomalies mostly in central Europe with a return period of about 50 years in observational records. Major impacts were seen in multiple countries and the joint investigation of hydrological and meteorological drought,

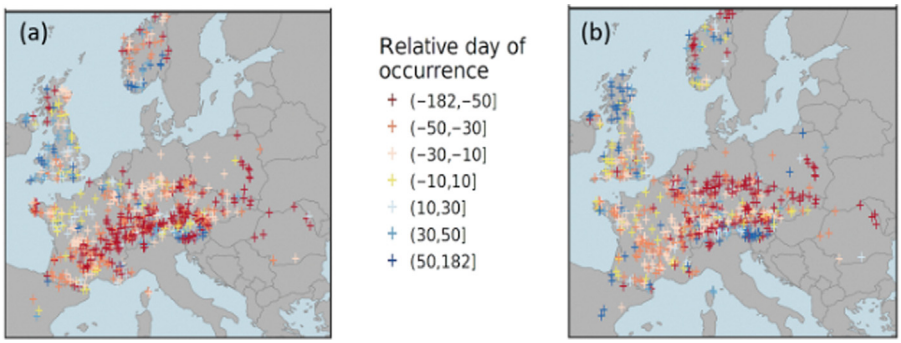

FIGURE 11.4

Relative day of occurrence of the onset of the river flow drought events of: (a) 2003 drought, and (b) 2015 drought, as compared to the benchmark period.

Modified from Laaha et al. (2017).

including their dependencies, facilitated a better understanding of their cause (Van Lanen et al., 2016). Another interesting finding is the change in the relative day of onset of the two hydrological droughts as compared to the benchmark (Fig. 11.4). In 2003, the hydrological drought started 50−182 days earlier (red crosses) than in the benchmark period in a zone from southern France to Austria over Switzerland. In 2015, a similar earlier onset (red crosses) was seen in a more northern zone stretching from Luxembourg to Slovakia over southern Germany and the Czech Republic. Earlier occurrences (red) related to relatively drier preconditions in winter or spring. Later occurrences (blue) related to relatively wetter preconditions. Overall, drought developed earlier and became more severe in regions with dry preconditions, whereas it developed later and was less severe in regions with wet preconditions.

Bakke et al. (2020) evaluated the extremely warm and dry 2018 summer drought in northern Europe. Streamflow drought developed in the Nordic region in June and in July with 68% of the stations experiencing record or near-record low river flow as compared to the period 1959−2018. Groundwater showed similar record low conditions in July and August (Nordic region). Extreme conditions persisted further south towards the end of the year and sustained longer in wells of increasing depth and associated longer response time. The authors highlight the delayed response in groundwater drought, which is important to take into account when analysing drought propagation and impacts of groundwater drought (Section 3.3.4.3).

Identifying causes and drivers of these extreme events may help improve drought predictability, which is vital for drought early warning (Chapter 13). Overall, a historic perspective, such as demonstrated by the examples given above, provides guidance on the severity of the drought and the frequency with which to expect droughts of similar magnitudes and extend in the future given a stationary climate.

11.3.3.2 Drought derived from simulated hydrological time series using reconstructed meteorological data

In the previous subsection, we presented some key hydrological droughts derived from observed time series of hydrometeorological data. Here, we add to this by including examples of studies based on

insufficient data, where data rescue and reconstruction were used (second approach, Section 11.3.2.1). The reconstruction of time series can be done using many different methods and techniques, and it is advised to use as many observations as possible to reduce the uncertainty in these reconstructed series.

In the studies by Smith et al. (2018) and Barker et al. (2019), a reconstruction of droughts in the United Kingdom was done for the period 1891−2015 (Section 11.3.2.1). Smith et al. (2018) reconstructed river flow back to 1891 for 303 catchments using a multi-objective calibration approach in combination with a hydrological model. The hydrological model was forced by rescued and digitised meteorological data from weather stations that archived observations in paper records. Model performance was assessed across the flow regime, including specific drought and low flow indices and its ability to reproduce historic drought events. Barker et al. (2019) used a subset of 108 near-natural catchments modelled by Smith et al. (2018), that is, stations particularly suitable for low flow, to identify and characterise historic hydrological droughts based on monthly time series of the Standardised Streamflow Index (SSI) for 3 and 12 month accumulation periods (Section 5.5). Identified drought events were ranked according to four event characteristics derived from consecutively negative SSI values (i.e., duration, accumulated deficit, mean deficit and maximum intensity). Events with a duration of less than three months were removed. The additional data provided by the reconstructions meant that events of the recent past (i.e., the last 50 years) could be placed in a historic context. They found the 1976 drought to be a more severe hydrological drought event than more recent drought episodes. So-called heat maps, which show the drought severity as a function of time, were used for visualisation purposes. Heat maps allow for a visual comparison of a phenomenon in two dimensions, here drought patterns in space and time, where on one axis, catchments are listed from north to south in the UK and on the other axis, time is given in years (Fig. 11.5). By colouring the matrix for (the degree of severity of) a drought characteristic of your choice, one can obtain geographical patterns in drought characteristics over time. This spatial comparison based on a standardised drought index also allows you to detect coherent drought regions, as Barker et al. (2019) did in their historic drought reconstruction. Overall, it is highly recommended to assess drought characteristics in a historic perspective, if possible, to view current trends in the context of long-term variability, as well as in a regional context to detect consistent change patterns in space.

11.3.3.3 Drought derived from simulated hydrological time series using large-scale hydrological models and gridded meteorological forcing

Studies on historic hydrological drought derived from simulated time series of hydrological data (river flow or groundwater) using large-scale models forced by gridded meteorological forcing are manifold (third approach, Section 11.3.2.2). Fig. 11.6 provides one such example outcome. The map gives the total number of drought events over a 28-year period for major European rivers. The LISFLOOD (Burek et al., 2013, Table 9.2) was used to simulate time series of historic daily river flow for each river node using a 5 km spatial resolution. The gridded meteorological data, which serve as input for LISFLOOD, were derived from ground observations (>5000 synoptic stations). The simulated daily flow in each river node was then aggregated to monthly totals, and hydrological drought was determined for each river node using the Standardised Streamflow Index (Section 5.5) with an accumulation period of 1 month (SSI-1). Eventually, the total number of drought events was mapped (Fig. 11.6). A low number (e.g., on average < 1 event per year, mapped as green), is seen, for example, in the Iberian Peninsula. Higher numbers (e.g., an average > 2 events per year, mapped as orange or red) are found in

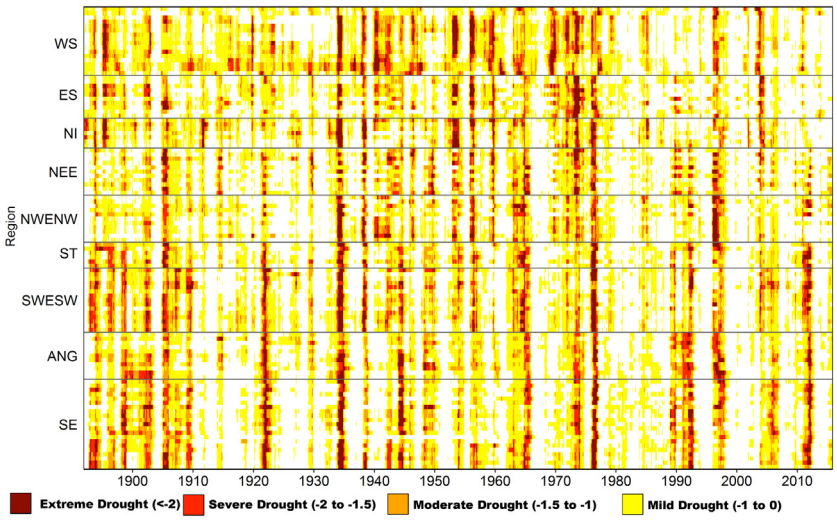

FIGURE 11.5

Drought in river flow in the UK illustrated using heat map of SSI-12 from 1891 to 2015. Drought severity for near-natural catchments, arranged roughly from north to south on the y-axis (hydro-climate regions), with one row per catchment, is classified into four classes based on the SSI-12 value. West Scotland (WS), East Scotland (ES), Northern Ireland (NI), Northeast England (NEE), Northwest England and North Wales (NWENW), Severn-Trent (ST), Southwest England and South Wales (SWESW), Anglian (ANG) and South England (SE).

Modified from Barker et al. (2019).

FIGURE 11.6

Number of droughts in European rivers from October 1990 to September 2018 (29 years) identified using the Standardized Streamflow Index (SSI-1). Smaller rivers are not shown.

Modified from Sutanto and Van Lanen (2021).

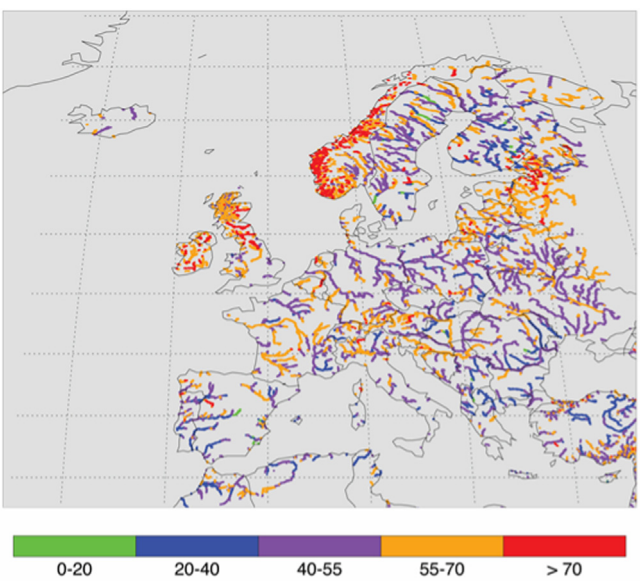

regions along the Norwegian coast, the United Kingdom and Ireland and northeast of the Baltic countries. A high number of events implies a flashy hydrograph and short duration droughts.

Many large-scale hydrological drought studies, which use the outcome from large-scale models forced by gridded meteorological data, have been done in the context of Model Intercomparison Projects (MIPs), including WaterMIP (Haddeland et al., 2011) and ISI-MIP (Warszawski et al., 2013), (Section 9.4.2). A MIP for the historic period primarily aims to investigate the performances of a set of models by comparing their performance against observations, and the models against each other. The model evaluation for the historic period then serves as benchmark for drought projections. In WaterMIP, which was part of the EU WATCH project (Harding et al., 2011), 11 large-scale models (Table 9.2) were included. A consistent simulation setup was used for all models and the WATCH Forcing Data (WFD, Weedon et al., 2011) was used as input. All models were run at 0.5° spatial resolution for land areas across the world and simulated time series of daily runoff obtained for the historic period 1963–2000 for each land grid cell. This ensemble of simulated historic time series has served as the starting point for a number of global and regional scale drought studies, as exemplified below for four studies. A common focus of these studies is an assessment of the models' ability to capture historic droughts and in this way to explore the credibility of the models to assess future drought (Section 11.4).

The first of these studies, Prudhomme et al. (2011), included three of the global WATCH models with the aim to investigate the ability of gridded hydrological models to reproduce regional-scale high and low flow events in 23 regions across Europe. The comparison was done for a catalogue of historical droughts derived using the Regional Deficiency Index (RDI, Section 5.7.1). The RDI was derived from observed river flow across Europe, and the same method was applied to time series of simulated runoff for the period 1963–2001. Observed and simulated RDI time series were then compared using different performance measures, including the Spearman correlation coefficient (Section 7.3.2). The cumulative frequency distribution of the correlation coefficients for each of the models is shown in Fig.11.7.

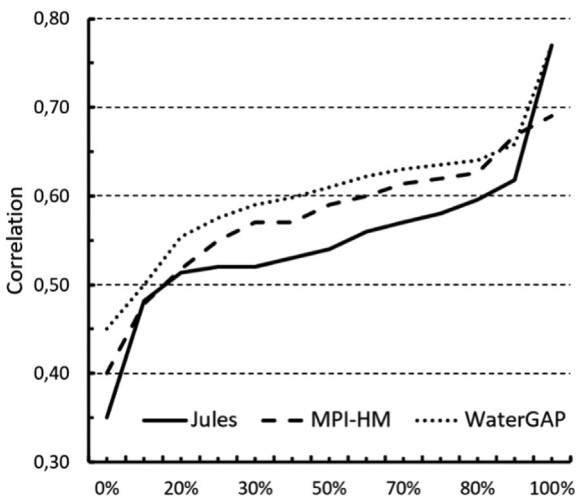

FIGURE 11.7

Cumulative frequency of the correlation (Spearman correlation coefficient) between observed and simulated RDI (Regional Deficiency Index) for three large-scale models (Jules, MPI-HM, WaterGAP, Table 9.2) covering 23 homogeneous regions in Europe.

Derived from Prudhomme et al. (2011).

The correlation between observed and simulated RDI varies between regions (not shown). One can also notice that the cumulative frequency distributions of the models follow approximately the same pattern. The Jules model has the largest variation in the correlation coefficient across the regions (0.35−0.77). The highest correlation is found for all three models in southeast Great Britain (0.63−0.77), an area characterised by slowly responding catchments because of extensive groundwater bodies. The lowest correlations (0.35−0.45) are seen in mountainous regions (e.g., Pyrenees, French southern Alps). It is likely that rather coarse spatial resolution of the models and the climate forcing data (0.5°) do not adequately capture weather and hydrological processes associated with the highly variable topography of these regions. The results showed that differences between the various model outputs and observed data existed and should be considered in interpreting future drought derived from these models. However, the results presented by Prudhomme et al. (2011) suggest that overall global models could be expected to provide realistic future drought characteristics in Europe.

Gudmundsson et al. (2012) compared time series of simulated runoff from an ensemble of nine global models (from the WATCH project) against observed river flow from more than 400 hundred small, near-natural catchments in Europe. Most catchments were considerably smaller than the grid cells (on average 10%−25% of the grid cell area), which implied that several grid cells contained more than one catchment. In this case, either the average, or the catchment covering the larger part of the grid cell, was chosen. This resulted in 293 cells with paired series of observed river flow and simulated runoff. Models were evaluated with respect to their ability to capture the interannual variability of spatially aggregated annual time series of five runoff percentiles (derived from daily time series), including annual low and high flow. Eventually, spatially aggregated annual time series of observed and simulated runoff percentiles across Europe were plotted for five percentiles, here the Q_{95} and the Q_{75} are shown (Fig. 11.8). Please note that we use the hydrological definition for the percentiles (i.e. flow exceedance) here (Box 5.1), as opposed to the study by Gudmundsson et al. (2012).

Overall, the models captured rather well the interannual variability of the observed runoff for both the Q_{75} (Fig. 11.8a) and the Q_{95} (Fig. 11.8b). However, the ensemble spread (amplitude) was large for both percentiles and most models tended to underestimate the observed runoff (thick blue line), in particular for Q_{75} (Fig. 11.8a). Overall, errors in the mean and standard deviation as well as differences in performance between the models, increased for low percentiles (e.g., Q_{75}, Q_{95}), reflecting the

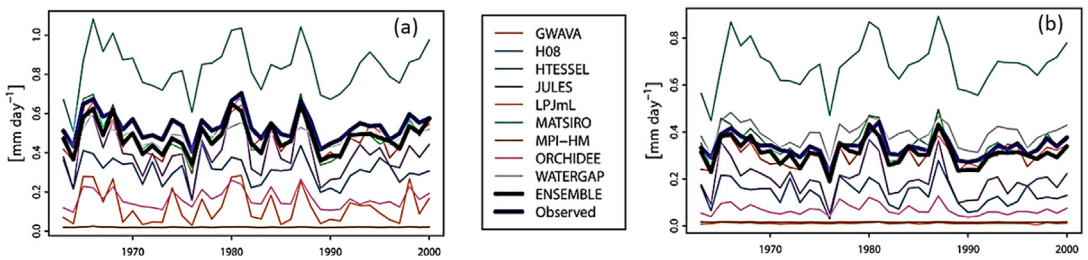

FIGURE 11.8

Annual time series of runoff percentiles for observed river flow and simulated runoff (for nine models and the model ensemble mean) in 293 grid cells with paired data over the period 1963−2000: (a) 75th percentile, Q_{75}, and (b) 95th percentile, Q_{95}.

Modified from Gudmundsson et al. (2012). © American Meteorological Society. Used with permission.

uncertainty of large-scale models in representing subsurface hydrological processes vital for sustaining low flow.

Van Huijgevoort et al. (2013) used an ensemble of ten global models (from the WATCH project) to analyse the temporal development of area in drought for 20 regions across the world. Droughts were identified by applying the Q_{80} threshold (Box 5.1) to simulated time series of runoff. They found the model ensemble spread (area in drought) to be largest in regions with low runoff (e.g., Sahara and adjacent regions) and smallest in regions with high runoff (e.g., Amazon, southeast Asia). They also observed a rather small spread in most regions in Europe, northern Asia and eastern United States. To obtain more insight in drought propagation (Sections 3.3–3.5), they also investigated the correlation between the area in drought derived from monthly aggregated precipitation (1, 3, 6 and 9 months) and the area derived from the ensemble median runoff. The highest correlation was found in regions with high runoff values, implying that drought propagation does not lead to substantial differences in the dynamic behaviour between meteorological and hydrological drought in this case. In drier regions, the opposite is observed (low correlations) meaning that differences in temporal patterns between meteorological and hydrological drought are pronounced. Corzo Perez et al. (2011) used the same set of global models to investigate the development of the area in drought across the globe, but adding the spatial coherence of drought, that is, contiguous drought areas were identified over time (Section 5.7.2). An areal threshold (minimum number of neighbouring cells in drought) was introduced to identify drought clusters. They found that in the period 1976–2000, the number of drought clusters varied from about 500 to 850 across the world (similar to the heat map in Fig. 11.5).

The fourth and last example is based on an ensemble of seven global models (from the WATCH project) with the aim to evaluate their ability to map spatial and temporal patterns of large-scale droughts in Europe (Tallaksen and Stahl, 2014). The study used the same dataset as described by Gudmundsson et al. (2012) with 293 grid cells having paired series of observed river flow and simulated daily runoff (1963–2000). The time series were first smoothed using a 7-day backward averaging and drought events then identified using a daily varying threshold (i.e., the 20% non-exceedance frequency of each calendar day). Two spatial drought indices were derived, that is, the mean annual drought area and annual maximum drought cluster area (Section 5.7.2). Annual time series of mean drought area revealed a consistent model behavior, whereas high model dispersion was seen in the weekly evolution of contiguous area in drought and its annual maximum (Fig. 5.17a). Comparison with the nearly 300 catchment-scale flow observations showed an overall tendency to overestimate the number of drought events and hence, underestimate drought duration. On the other hand, persistence in drought-affected area (weekly mean) was underestimated, noticeable for one group of models, suggesting that these models were too responsive and therefore not able to satisfactorily capture hydrological drought. The authors concluded that "an improved conceptualisation of the dynamic behavior of large-scale models, in particular the representation of stores and hydrological response, is vital to enable a better simulation of prolonged dry periods and extensive drought extent". Further, that one should be careful when using large-scale models for drought assessment at the catchment scale, especially if a single combination of only one hydrological model and one gridded meteorological dataset is used. Stahl et al. (2012) used an ensemble of eight global models (from the WATCH project) to fill in time series of historic river flow (runoff) at grid cells within Europe, where observed river flow data were missing (white space on the map). This enabled large-scale coherent patterns of river flow trends to emerge.

The studies presented herein demonstrate the added value and opportunities hydrological modelling provides in regions where no or limited observed data are available. Stahl et al. (2019) present a comprehensive overview of trends in historical hydrological drought in Europe, addressing available data, trends in observed river flow and simulated runoff and influence of decadal-scale variability in river flow time series. In addition, Hasan et al. (2019) present a systematic review of scientific papers on hydrological drought published since 2000. This covers, among others, an overview of major research themes addressed by these papers (e.g., drought severity, drought forecasting).

11.4 Future

11.4.1 Data availability

Knowledge on historical drought (Sections 11.2 and 11.3) provides valuable information to place ongoing as well as historic droughts in perspective, but it also helps to provide a historical benchmark for comparison to drought projections (i.e., droughts that may happen in the future). While droughts in the distant past and instrumental period can be characterised based on mainly observations, regularly in combination with models, we rely on modelled data only to provide projections. These projections are affected by different sources of uncertainty, as elaborated in Box 11.2.

Most projections are derived from GCMs or RCMs, which simulate, ocean, atmosphere and land processes at coarse spatial resolutions, for periods in the future (Sections 2.5.2 and 9.2). The spatial resolution ranges from 10 to 250 km, which makes it difficult to deploy the model output directly to regional and catchment scale modelling. Besides, these models have biases, which need to be addressed (Box 11.1) before using the data as forcing data for hydrological modelling purposes. To transfer these large-scale global projections to smaller spatial scales some sort of down-scaling and bias-correction techniques are needed to bring the data to the appropriate spatial and temporal resolutions (Section 11.4.2, Box 11.1).

As part of the Coupled Model Intercomparison Project (CMIP), which started in the 1990s, several groups around the world provide projections derived from state-of-the-art GCMs. The output from these models is publicly available and among others used by the Intergovernmental Panel on Climate Change (IPCC) to provide outlooks, among others for future droughts. The sixth round of CMIP (CMIP6) provides model results based on over 60 GCMs to predict future drought around the world (URL 11.2). Cook et al. (2020) used a selection of these GCMs to explore future meteorological, soil moisture and hydrological drought across the globe (Section 11.4.3). The CMIP projection data provide a good starting point when you want to study future drought in your area of interest. However, you should be aware of some limitations and issues that can occur when using these data sources. Below, some guidelines on which data to use as input and the limitation and potential of each data source are provided.

Firstly, you should be aware that simulation from the CMIP ensemble all follows so-called pathways. There are two types of pathways, shared socio-economic pathways (SSPs, Riahi et al., 2017) and representative concentration pathways (RCPs, Meinshausen et al., 2011). SSPs provide narratives describing alternative socio-economic trajectories that we will likely follow given certain economic scenarios describing the development of, for example, the Global Domestic Product (GDP), population, urbanisation and the related CO_2 emissions. These SSPs are strongly connected to the RCPs, which describe changes in atmospheric CO_2 concentrations and their related effect on the changes in radiative forces. The RCPs (RCP2.6, RCP3.4, … RCP8.5) are labelled after a possible range of radiative forcing values in the year 2100 (i.e., 2.6, 3.4, …. 8.5 W m^{-2}). They provide a range of potential climate impacts based on carbon emission policies and the evolution of contrasting, but

realistic political-economic philosophies. All GCMs included in a CMIP effort simulate the different combinations of pathways resulting in a set of simulations (ensemble) with climate change impacts ranging from minor to severe depending on the scenario you select. It is always a good idea to explore several possible scenarios to get a good estimate of the uncertainty related to the different climate projections.

Some studies use directly the output from GCMs (e.g., time series of gridded runoff) to derive future drought characteristics (e.g., Arnell, 2003). These studies have a coarse spatial scale (e.g., 1.5°, Cook et al., 2020) and provide not more than a first global perspective. Hence, it should be complemented with investigations on a more detailed scale. Such more detailed studies commonly use downscaled and bias-corrected time series of gridded meteorological data for the future (Box 11.1), which serve as driving force for hydrological modelling. Examples are the WATCH dataset (Weedon et al., 2011), the ISI-MIP dataset (Warszawski et al., 2013) and WFDE5 dataset (Cucchi et al., 2020), which all contain bias-corrected meteorological data from several GCMs and a number of emission scenarios or RCPs. This removes the need to perform your own downscaling and bias-correction, but the spatial resolution of these projections is still rather coarse for most catchment-scale studies.

In an assessment of drought projections, it is valuable to look at the effect of using different GCM input data in combination with a set of hydrological models, as this will provide you with valuable information on the uncertainty and limitations of your projections (Box 11.2). In order words, to perform a multi-GCM, multi-hydrological model analysis for a certain RCP or SSP. The performance of an ensemble of model simulations driven by different forcing datasets can be evaluated based on historic data (e.g., time series of meteorological data derived from observations or from downscaled, bias-corrected output from climate models). You can follow similar approaches as those studies described in Section 11.3.3, which all evaluate the performance of several off-line large-scale model in their ability to capture large-scale drought behaviour in Europe as identified from observations. A range of performance statistics, such as mean, standard deviation and serial correlation (Section 6.5.1.1), provide valuable information on the reliability of these large-scale approaches for drought projections. Models that adequately perform in the past are thought to be more credible in their simulation of future drought, although some uncertainty still remains.

11.4.2 Methods to identify future drought

It is important to be aware that climate projections are affected by biases. As a result (first step in the assessment of future drought), most models provide a simulation of the historical period (benchmark period, for example, 1981−2010 or 1991−2020), which can be used to quantify the biases. Simulations for the future period are then corrected using some sort of bias-correction procedure (Box 11.1). The benchmark is sometimes called baseline or reference period. It is common to assume that the biases are similar for the historical simulations and the projections, which allows you to correct the projections based on the error characteristics of the historic simulations. Therefore, it is important to always consider the following two points when using climate projections:

(a) validate for (downscaled) projections, using either a dynamic (GCM-RCM) or a statistical (GCM-SDM) downscaling over a recent period (benchmark period) against local observations in terms of climate statistics

(b) reiterate with alternative large-scale forcing datasets for assessing the associated uncertainties in the future climate, using: (a) different GCMs (to assess the effect of GCM uncertainty), (b) different runs (perturbations) of a GCM (to assess the impact of the GCM internal variability), and (c) different emissions scenarios (RCPs or SSPs).

In general, two approaches exist for simulating future hydrological drought using a hydrological model in combination with climate projections from large-scale climate models:

(a) top-down, scenario approach, where the output from climate models (GCMs or RCMs) and their downscaled results are used as input to hydrological models and associated simulations analysed
(b) bottom-up, scenario approach, where several hydrological model simulations (often hundreds to thousands) are performed bounded by the variation in a range of key meteorological variables (typically, based on perturbed observation time series of observed meteorological data or stochastic weather generators; Guo et al., 2017).

The advantage of directly using the output from large-scale climate models (top−down) is that the consistency and correlations between the different meteorological variables are maintained (e.g., solar radiation, 2 m air temperature). For meteorological variables, where shifts in the diurnal cycle or spatial patterns are observed, these shifts are more easily reflected by the use of large-scale climate models as they simulate the fully coupled atmospheric system, which ensures that correlation and covariance between the different meteorological variables are maintained. A disadvantage of this approach is that often the data require some form of bias-correction and post-processing (Box 11.1) before it can be used in hydrological modelling, which would require additional work.

The bottom-up approach has the advantage that observed data can be used and changes can be applied directly to these time series. For example, simply adding 2°C consistently to an air temperature time series (referred to as the delta change approach). The method is simple and requires limited computational effort. As the original data come from the observational record, no bias corrections or downscaling are applied, and covariances and other statistical properties in the data are preserved. The disadvantage of this approach is that it may be too simplistic to simply correct for the changes, and second-order properties of the time series may change as well (e.g., diurnal cycle, clustering of rain events). Further, physical relationships may be broken (e.g., raising air temperature add 2°C without correcting the evaporative demand) as discussed by Haddeland et al. (2012).

Which method is the most appropriate depends on the application and research question of interest. Considerations include the performance of the modelling chain to reproduce hydrological extremes and in particular low flow conditions (e.g., Prudhomme et al., 2014; Giuntoli et al., 2015, Section 11.3.3), but various models or model chains often show mixed patterns with performance varying over seasonal and geographic regions. Top-down approaches are most widely used. Typical for this type of projections is that they provide pathways forward rather than exact predictions of when a future drought will occur. The goal is to provide general climate characteristics and not predict the exact timing of future drought events as done in forecasting (Section 13.4). The climate projection data provide possible weather patterns for the future, which can then be used to derive drought characteristics. This makes projections suited to detect changes and long-term trends in drought characteristics.

The workflow presented in Fig. 11.2 can be followed in the top-down approach (direct use of climate data from GCMs or RCMs). The workflow applies to a single hydrological model, but can also be applied to an ensemble of large-scale models (GHMs or LSMs, Table 9.2). However, a severe limitation of these larger-scale models is that they cannot resolve high-resolution processes linked to, for example, steep altitude gradients and related snow processes. Providing catchment-scale projections from global-scale (gridded) projections add some additional challenges. For example, the spatial representativeness of the river network from these global projections does not always reflect the

local topography and the influence of local water management is often ignored. Modelling frameworks targeted at a more detailed scale allow for projections that can be used as inputs for dedicated adaptation strategies in terms of water resource management in general and drought management in particular (Sauquet et al., 2016). This is especially relevant in catchments that are heavily impacted by human interventions (e.g., large infrastructures – such as multipurpose reservoirs or water transfer facilities), whose operations have a considerable influence on the water availability at a given time, including low flow, and at a given point in the catchment (Section 10.3).

Box 11.2 Quantifying uncertainty using ensemble modelling

Model uncertainty can be quantified by using ensembles, that is, by considering not just a single simulated time series from which the drought events are derived, but by allowing for multiple time series. You can achieve this implementing a combination of: (a) initial condition perturbation, (b) multiple parameterisations, and (c) multiple models.

Initial condition perturbation

This is critically important in atmospheric modelling and forecasting and was the first type of ensemble modelling to be developed. Here, a single model is used, with slightly different input or initial conditions (called perturbed conditions) to account for uncertainty in the observation data and its propagation through the models, also called 'initial condition uncertainty'. Inputs could be states, such as the initial vegetation cover and soil moisture conditions. This approach is primarily relevant for climate models, that is, models whose weather simulation paths heavily depend on initial conditions because of the chaotic properties of the atmospheric system, but the concept can also be applied in hydrological modelling for different initial states (Section 9.2.3 and Box 9.4).

Multiple parameterisations

Hydrological models, in particular lumped hydrological models (Section 9.3), rely on a number of model parameters whose value cannot be measured directly, as they aim to describe several physical processes in a single parameter. The parameters are defined by minimising errors between the simulated variable (e.g., river flow) and its observation, using either the parameter set achieving the smallest error or the range of parameter sets that achieve a maximum acceptable error (Beven and Freer, 2001, Sections 7.3.4, 7.3.6, 9.3.2 and 9.4.2). Depending on the error measure chosen (also called objective function) different parameters sets with a similar performance can be found, and calibrations based on multiple parameters sets have also been advocated (Smith et al., 2018). When focus is on low flow and hydrological drought, objective functions aiming to reduce errors in the lower part of the hydrological distribution are often favoured. One option to quantify the uncertainty caused by the parameter set is to run an ensemble of models that all have relatively good model performance. This will provide you with an envelope of possible solutions at any given timestep and give valuable information of the uncertainty that is inherited from the parameter variability.

Multiple models

Because of the simplified representation of hydrological processes by hydrological models, and because different models include different processes, it is recommended to use several models having different model structures to capture process uncertainty. The technique was first implemented in the climate model community to generate climate projections and is now commonly applied in the water sector (multi-model experiments). Possible implementations include multiple models run for the same catchment (Veldkamp et al., 2018) or modelling frameworks, where one can replace parts of the model, for example, the snow routine (Melsen et al., 2019). For larger spatial scales, these efforts often rely on a community effort, with many modelling groups adhering to a common modelling protocol so that simulations are comparable and can be analysed jointly (Haddeland et al., 2011; Warszawski et al., 2013). In all cases, the spread among the models provides information about the influence of modelling structure on the results. Running multi-model ensembles (at any scale) is relatively time-consuming; however, it does provide much needed information, especially when it comes to projections. As we do not know how well different model structures capture possible changes in meteorological and hydrological processes, the use of several model structures provides important information of the inherited uncertainty in model structure and parametrisation. With climate change, some physical processes may change, and this will be simulated differently by the ensemble of models. Therefore, future simulations nowadays commonly rely on multi-climate, multi-hydrological model ensembles to make reliable projections of future hydrological drought, including uncertainty estimates (Vidal et al., 2016).

11.4.3 Drought in the future

As the Earth continues to warm due to climate change, it is generally expected that drought occurrence and severity will increase in parts of the world (Caretta et al., 2022). Many studies have looked at the projections of drought, all using slightly different GCM input data or hydrological modelling tools. However, there is a strong consensus among most studies on the direction of change and regions facing an increase in drought risk. Independent on the scenario and models used, most studies agree that we will observe an increase in drought risk for the Mediterranean, large parts of South America, Southern Europe, parts of the United States, Africa and Australia (e.g., Prudhomme et al., 2014; Wanders et al., 2015; Cook et al., 2020). These general patterns are present in most studies looking at drought and are found to be robust.

Cook et al. (2020) investigated 21st century drought across the globe based on 13 GCMs and five SSPs from CMIP6 at a 1.5° spatial resolution. Drought in precipitation, soil moisture and runoff were identified by the end of the century (2071−2100) relative to a preindustrial benchmark (1851−80). Droughts were directly drawn from the GCM time series. Runoff was averaged over six months' periods (April−September and October−March). One index studied was the occurrence of extreme single-year drought events, that is, events when runoff was below or equal the Q_{90} (Box 5.1) of the benchmark runoff. They found extreme single-year drought to occur in the above-mentioned regions up to 3 to 4 times more than in the preindustrial period. As expected, the increase in single-year drought was greatest in the higher warming scenarios (RCP8.5). Cook et al. (2020) did not use any downscaling or bias correction, thus being a rather coarse approach.

While additional GCMs projections, hydrological models, and downscaling and bias correction methods will become available in the future, we expect that the dominating spatial patterns in drought behaviour as reported below will sustain in future studies. However, the exact effect on individual regions and catchment may vary depending on its climate and physiographical characteristics, although the direction of the signal is unlikely to change.

11.4.3.1 Example of future drought at the global scale using different benchmark periods

Wanders et al. (2015) studied future drought at a more detailed scale using a global hydrological model (PCR-GLOBWB, Sutanudjaja et al., 2018, Section 9.4.2). The PCR-GLOBWB model was forced by an ensemble of GCMs from CMIP5, known as the ISI-MIP ensemble (Warszawski et al., 2013). The ISI-MIP ensemble contains bias-corrected precipitation and temperature estimates for the period 1970−2099 for five GCMs and four RCPs. This ensemble of climate data comprises in total 20 realisations (GCM-RCP combinations) of daily time series of gridded runoff at 50 km spatial resolution, resulting in a total of 67,420 simulated runoff time series across the world.

A global analysis requires that one accounts for local hydrological conditions, such as intermittent rivers or regions permanently covered with snow and ice, as hydrological models typically will always produce some groundwater discharge. The drought characterisation methods should also be able to deal with the different hydroclimatic conditions found across the world. In this study, drought events were derived by the threshold-level approach. After determining the daily variable threshold (derived from monthly Q_{90} thresholds applying a centred 30-day moving average), drought characteristics (duration and deficit volume) were obtained (Section 5.4.1).

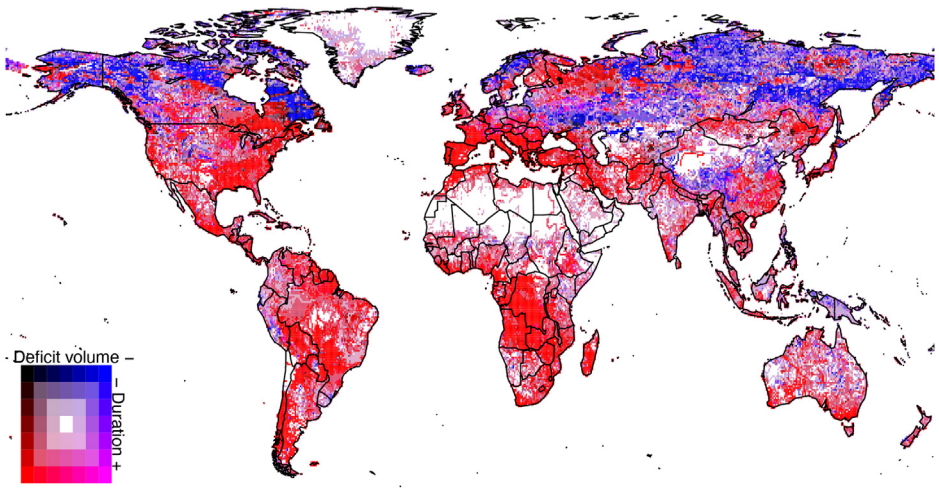

FIGURE 11.9

Robustness (number of models that agree on the sign of the direction of change) of drought in runoff (duration and deficit volume) in a future climate (+ means increase (*red colour*) in duration or deficit, and − means decrease (*blue colour*) in duration or deficit), under RCP8.5 simulated with the hydrological model PCR-GLOBWB forced by an ensemble of five GCMs for the period 2070–99. A non-transient benchmark period (1979–2000) was applied. More *saturated colours* indicate a higher degree of agreement in drought trends between the different GCM model forcing.

Modified from Wanders et al. (2015).

Drought characteristics were obtained from simulated runoff time series for all grid cells and selected combinations of GCM and RCP simulations. These data constitute the basis for Fig. 11.9, which shows the projected changes in drought deficit volume and drought duration based on the ensemble of model simulations, that is, the hydrological model PCR-GLOBWB run with the climate output of five GCMS for RCP8.5. As a first step, the threshold was based on the historical simulations from 1971−2000 (benchmark period), that is, a non-transient approach (Section 5.4.1). The average drought duration and deficit volume were calculated from the simulated time series of runoff in each grid cell for the periods 1971−2000 and 2070−99. Afterwards the direction of change, that is, increasing duration or deficit volume (positive +) or decreasing (negative −) was determined. Then, for the selected RCP8.5 and each grid cell, five directions of change were calculated (one for the output of each GCM). Robustness was derived from the agreement of the number of GCMs that were used as driving force, that is, the direction of change was considered: (a) robust: the change in drought characteristics derived based on all five GCMs agrees, (b) likely: the output from four GCMs agrees, and (c) plausible: the output from three GCMs agrees. The results were visualised through a bivariate classification that presents the trends in a coloured matrix (Fig. 11.9, lower left). Drought deficit volume is plotted along the horizontal axis and drought duration on the vertical axis. More saturated colours indicate a higher degree of agreement in the direction of change in drought (duration and

deficit volume) between the different GCM model forcing. For example, the grid cell is coloured red (lower left of coloured matrix) when all five directions of change in drought deficit and drought duration are positive, whereas the cell is coloured blue when both directions of change are negative.

In general, we see that if duration is increasing there is also an increase in deficit volume (red colours), as can be expected; when drought last longer they are also more likely to have a high deficit volume by the end of the 21st century under the RCP8.5 scenario. Decreasing trends mainly can be seen in the snow-affected climates (Northern Hemisphere). In the Southern Hemisphere, hardly any decreasing trends occur. About 25% of the total land area is projected to experience a reduction in drought duration and deficit volume relative to the period 1971−2005.

As a second step, the study also tested another concept, that is, a transient benchmark period, implying that a 30-year period preceding, the period of interest was chosen as benchmark. This was motivated by that a change in the hydrological regime will result in response to a warming climate. It is here hypothesised that society may adapt to the regime change, and hence, it may be useful to identify the droughts relative to the changed regime. It is then critical to also report the changes in the threshold itself along with the changes in drought characteristics. Application of a transient benchmark period, in this example, resulted in less severe droughts. Increased drought duration and deficit volume by the end of the 21st century is projected to occur on 27% of the global land area (RCP8.5) when the previous 30-year period is selected, which is substantially lower than using a non-transient benchmark period (62%, Fig. 11.9). The results based on a transient threshold may be more challenging to communicate to users than those based on a fixed benchmark period.

11.4.3.2 Example of future drought at the continental scale using multiple hydrological models

In the example above (Wanders et al., 2015), only one hydrological model was used (PCR-GLOBWB) instead of a recommended ensemble of hydrological models. The main reasons to work with only one single hydrological model is: (a) the availability and experience with the available hydrological models, (b) the high computational demands that are required to run an ensemble of hydrological models, and (c) the disability of some hydrological models to simulate certain processes. Using a multiple of models would normally require a community effort as demonstrated by various MIP efforts and collaborative studies, including researchers from different modelling groups. For example, Prudhomme et al. (2014) used five bias-corrected GCMs to force seven global hydrological models (Table 9.2) to study the influence of climate change on future hydrological drought (derived from gridded runoff). They calculated the Regional Deficit Index (RDI, Sections 5.7.1 and 11.3.3) for 17 large regions covering the world. The change in RDI (for each hydrological models) by the end of the century relative to the benchmark, is plotted in Fig. 11.10. Hydrological drought was found to most likely increase in large parts of the world. The signal was strongest in central Europe (CEu). The global hydrological models were rather consistent in the sign of the drying, except Jules (JUL), which is the only model that has a vegetation module. Jules reported a negative percent change (wetting, i.e., smaller future RDI) in all 17 regions. All other models (except PCR-GLOBWB, PCR for short), state negative percent changes in no more than 1−3 regions. Eastern Africa (EAf) was identified as the region with a negative change by almost all models. This implies that most of the models projected a positive percent change (drying, i.e., larger RDI)) for most of the regions. All models agreed on a positive change in central Europe (CEu) and mesoAmerica (MAm). The models also deviated in the magnitude of the percent change, with MPI and PCR-GLOBWB (PCR) having the overall largest

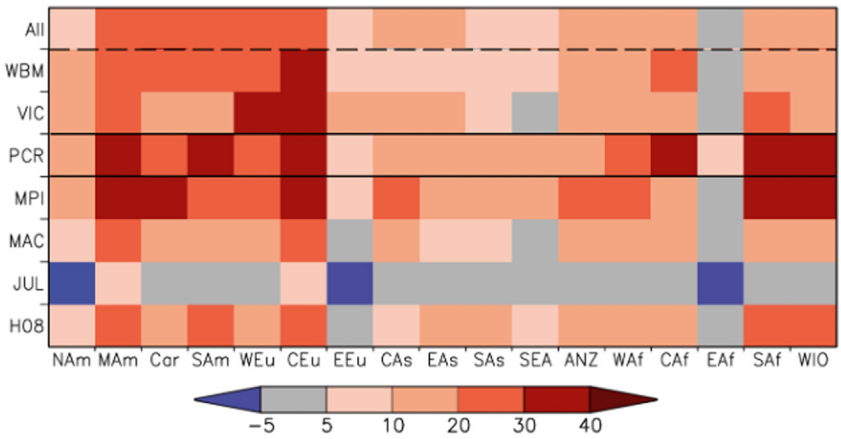

FIGURE 11.10

Future drought: Percent change in the Regional deficit Index (RDI) between the period 2070–99 and the benchmark period (1976–2005) derived with seven global hydrological models (*vertical axis*) for 17 regions across the globe (*horizontal axis*) and the RCP8.5 warming scenario. Values from each of the seven global hydrological models are average over the five GCMs and 17 regions, and 'All' is the average change over all five GCMs and seven global hydrological models. The regions comprise North America (NAm), MesoAmerica (MAm), Caribbean (Car), South America (SAm), Western Europe (WEu), Central Europe (CEu), Eastern Europe (EEu), Central Asia (CAs), East Asia and Northwest Pacific (EAs), South Asia (SAs), Southeast Asia (SEA), Australia and New Zealand (ANZ); Western Africa (WAf), Central Africa (CAf), Eastern Africa (EAf), Southern Africa (SAf) and Western Indian Ocean(WIO).

Modified from Prudhomme et al. (2014).

changes. The spread among the large-scale models (LSMs and GHMs) was found to be larger than that from the GCM projections alone (not shown).

Other studies looking specifically at hydrological drought in Europe have found similar patterns for the last 3 decades. For example, Marx et al. (2018) found a drying trend in low flow (i.e., Q_{90}, Box 5.1) in the Mediterranean and eastern Europe mainly due to decreasing annual precipitation (lower summer low flow), while an increase was seen in the Alpine and northern regions due to changes in snow accumulation and melt (higher winter low flow). Similar to the study by Prudhomme et al. (2014), Marx et al. (2018) deployed a combination of several large-scale GCMs and large-scale hydrological models to investigate hydrological drought over Europe — Marx et al. (2018) used simulated river flow rather than gridded runoff. Forzieri et al. (2014) explored future streamflow drought in Europe based upon a set of climate models (GCMs) and one hydrological model (LISFLOOD, Table 9.2). They showed the evolution of low flow and hydrological drought characteristics, respectively *MAM*(7-day) and deficit volume, over the 21 century. The *MAM*(7-day) is expected to decrease and the deficit volume to increase in southern and eastern Europe, which is in line with the projections presented by Prudhomme et al. (2014) and Marx et al. (2018). In addition, Forzieri et al. (2014) projected an increase in deficit volume in western Europe (e.g., France, Benelux, UK). All the three above-mentioned studies found seasonal differences in drought projections within Europe, where changes in snowfall

and increasing evaporation were found to influence these seasonal shifts. In regions where snow is the dominant form of winter precipitation, snowmelt in spring and summer substantially contribute to the summer discharge. With increasing air temperatures, snowmelt will occur earlier in the year potentially leading to more summer droughts.

11.4.4 Human interventions on future drought

In Chapter 10, we discussed the influence of human interventions on drought in the historic period. Such alterations to the hydrological system will continue in the future and thus will affect hydrology in the 21st century along with climate change. Human interventions are expected to increase further as developing countries are fostering more water-related infrastructure, such as reservoirs, irrigated fields and increased abstractions for industrial and domestic water use. This will have a notable influence on the hydrological cycle as these measures will all affect the river flow, either by altering the flow regime (reservoirs) or changing (likely increasing) the use of water in the catchment (irrigation and water abstractions) as elaborated in Section 10.3. At the same time, a change to more sustainable water use may to some degree counteract this development.

It is projected that water-related infrastructure expansion mainly will occur in developing countries, where population growth and an increase in economic welfare will drive an increasing need for water. To sustain growing populations and increase economic welfare, one has seen a rapid expansion of irrigated lands in India and other parts of Asia. This in turn has had an impact on the use of water to sustain these activities.

Another impactful measure is the construction of reservoirs that are used for various purposes, ranging from flood control, to water supply and low flow augmentation (Section 10.3). Currently, most reservoirs can be found in North America, Europe and in recent years Asia. Future expansions are mostly expected to occur in Asia, South-America and Africa (Gernaat et al., 2017). These regions have a large reservoir potential, while the number of constructed reservoirs is still low. Likely, the growing population and economy will call for reservoir construction. Clearly, these reservoirs will have a significant impact on future discharge in major rivers.

Land use is another human influence that is expected to have a major impact on the future hydrological cycle. SSPs (Section 11.4.1) do not only describe the socio-economic changes, but also the associated changes in land use. For example, deforestation in favour of (irrigated) cropland is expected to reduce the water holding capacity of the catchment and result in a stronger seasonality and higher storm runoff. More densely forested areas reduce direct runoff and thus decrease the peak discharge during precipitation events (e.g., Guzha et al., 2018).

These and other human interventions must be taken into account when assessing future droughts and their potential impacts (Wada et al., 2017). As the future is largely unknown it is difficult to predict which human influences are going to be dominant in a given region and the cascading effect it may potential have on the hydrological cycle. However, modelling these effects and their impact on the hydrological cycle provide a way forward and although challenging and associated with high uncertainties, it can provide valuable information to increase preparedness, drought adaptation and policy-making.

The combined influence of climate change and future human interventions can be assessed by seeking to quantify the impact of human water use and management on drought characteristics. For example, Wanders and Wada (2015) applied the global hydrological model PCR-GLOBWB

(Sutanudjaja et al., 2018) to simulate global hydrology with and without two common human interventions (i.e., irrigation and reservoirs) at a 0.5° spatial resolution for the RCP8.5 scenario. This resulted in two global simulations, where they specifically focussed on simulated daily river flow. The natural flow simulation was used to compute the daily (30-day moving average) variable threshold (Q_{90}, Box 5.1) in the absence of human interventions. The benchmark was then applied for the human intervention scenarios using a transient benchmark period (Section 11.4.3.1). By running simulations with and without human interventions, we can isolate the effects of climate change and human interventions. This can allow you to quantify where droughts would likely be alleviated and worsened due to these interventions (Fig. 11.11). Such a model exercise may also help identifying to which factor (natural or human intervention) changes in hydrological drought can be attributed.

The global map (Fig. 11.11) shows the impact of future water use and reservoirs on projected drought in river flow by the end of the 21st century. Hydrological drought is projected to increase in several regions across the world because of climate change (Figs. 11.9 and 11.10). Future water use and reservoirs are likely to amplify (or aggravate) (Fig. 11.11, brownish colours) hydrological drought in a zone stretching from western United States over northern Africa, the Mediterranean, Middle East, central Asia to China. There are also regions where the projected increase in hydrological drought due to climate change (i.e., drought becomes more severe), is projected to decrease (be alleviated) in response to the human interventions (Fig. 11.11, blueish colours), for example, in southern Africa, central and eastern Europe.

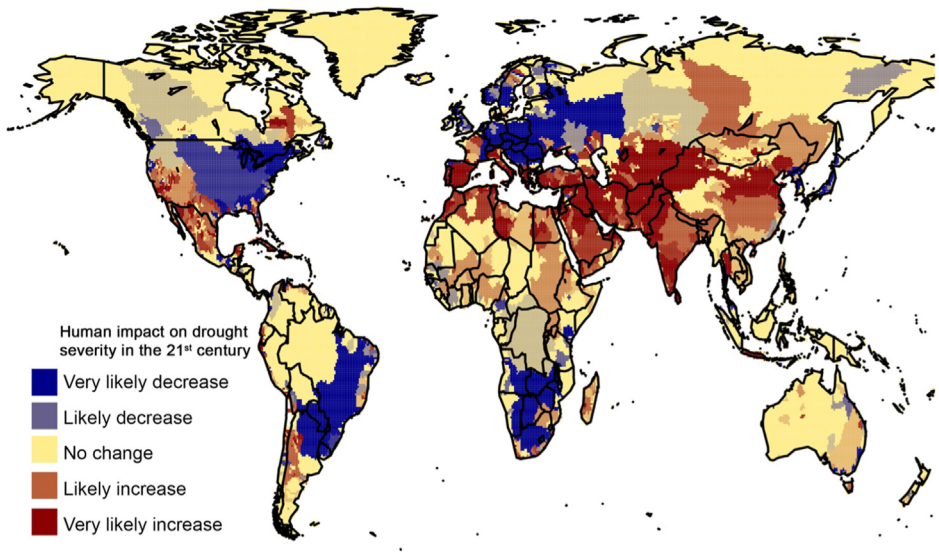

FIGURE 11.11

Influence of human interventions (reservoirs and human water use) in the summer (JJA) on future drought deficit volume (2070–99) under the RCP8.5 scenario using PCR-GLOBWB forced by five global climate models (GCMs). The transient benchmark period was applied to identify drought using the Q_{90} threshold.

Modified from Wanders and Wada (2015).

The effect of future water use on low flow and hydrological drought was investigated by Forzieri et al. (2014) for European rivers (Section 11.4.3.2). They simulated the combined effect of climate change and water use (water withdrawal and consumption in different sectors) on future drought (deficit volume) in 2080, as well as the effect of water use only. It must be stated that the withdrawal and consumption scenarios, in this and any other study, are also storylines of possible futures that are the result of policy decisions to be made in the future. In most European administrative regions, water use is expected to increase in the 21st century, except the southern Mediterranean (e.g., South Spain, South Italy, main parts of Greece). This is because of the projected reduction in irrigation water use. The combined effect of climate change and water use leads to the well-known dipole in Europe, that is, projected lower deficit volumes in Scandinavia and northeast Europe by the end of the 21st century and increased deficit volumes in the Mediterranean, central and west Europe (Fig. 11.12a). As expected, the effect of increase in water use only (Fig. 11.12b) translates into larger deficit volumes in several rivers in 2080, particularly in a zone stretching from the Adriatic Sea to the Black Sea (Balkans) and northwest Europe (Germany, Benelux and northwest France). Notable differences are seen in projected effect of human interventions between the continental analysis for Europe (Fig. 11.12b) and the global analysis (Fig. 11.11). The results are, however, not directly comparable due to the use of the Q_{90} as threshold and a transient benchmark period in the global analysis (Fig. 11.11) as compared to the Q_{80} and a benchmark based on the period 1961–90 for the European study (Fig. 11.12). In addition, other aspects add to the deviation, such as the spatial resolution, the hydrological variable (runoff in the global study versus river flow in the European study), different set of climate models, different hydrological models and different human interventions (reservoirs and water use versus water use only). This highlights the need for a careful analysis of all steps in a study is a needed before any comparison or conclusion can be made.

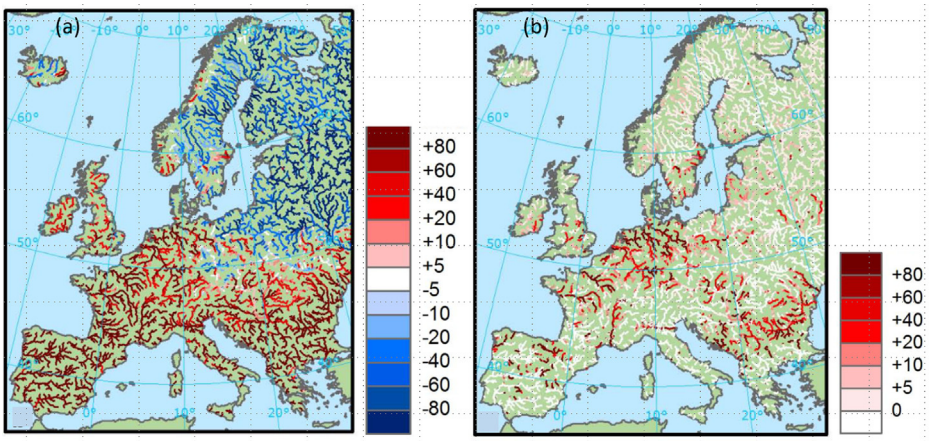

FIGURE 11.12

Ensemble-average change (%) of deficit volume in European rivers in 2080 relative to the benchmark (1961–90) due to: (a) climate change and water use, and (b) only water use.

Modified from Forzieri et al. (2014).

You can find a comprehensive overview of future drought in Van Lanen et al. (2019), which presents a review of drought projection studies. For example, they address future low flow and future hydrological drought across climate regions in the world, including uncertainties. They also describe hotspots of future drought (e.g., the Mediterranean Basin, Central America and Mexico, northern South America, South-West Argentina, Chile).

11.5 Summary

Studying drought on decadal timescales is challenging, but we can gain important knowledge from studying hydrological drought across time, here including the distant past, instrumental period and future. Historic records are obtained using either proxy observations (distant past), observations (instrumental period) or climate models (future) constrained by observations in the development stage. As the observational records of hydrometeorological data are expanding over time, we keep on adding to existing records and thereby gain new insight. As drought is by nature an extreme and thus rare phenomena, additional observations can help us to advance our knowledge of extreme drought events and thus improve our understanding of the variability, dominating trends and drought generating processes. This understanding is vital when we want to understand the underlying climate and catchment processes that determine hydrological drought characteristics in both the past and future. Having a better understanding of drought generating mechanisms, including the influence of human interventions, will aid efforts to understand decadal and centennial trends in hydrological drought, important to understand the impact of socio-economic changes around the world.

Long records are critical when we want to look at the natural climate variability compared to the enhanced climate signal. From the historical record (distant past and instrumental record, Sections 11.2 and 11.3), we can determine what level of outliers is expected given the full historic record. When (current) observations or projections indicate that the signal is moving away from the normal variability, society have the opportunity to react. To be able to detect trends or rapid changes in the drought signal we must have a sufficiently long record to be able to reliably quantify extremeness of these drought events. Accordingly, it is essential to combine records of past and future drought to centennial-scale drought records, which enable the long-term variability and trends to be assessed. In the case of hydrological extremes and drought in particular, it is important to have long records to recognise trends and distinguish between extremes and outliers.

Large-scale climate and hydrological modelling data provide a valuable tool to reconstruct hydrological time series of the past and provide projection of future drought. We looked at the different steps that you have to take to obtain reliable future drought projections (Fig. 11.2) and discussed a variety of approaches that allow you to make drought projections at scales ranging from catchment scale to global scale. Land use change and human interventions add to the complexity of predicting future drought characteristics, and we provided examples of how to disentangle the climate signal from other changes.

You should now be able to design your own study to characterise droughts in the distant past, instrumental period or future. With the use of proxy-records, large scale observational datasets or climate data generated by climate models you can create well-designed scientific experiments to look at the impact of long-term changes in the climate on drought characteristics. It is important to ensure that the different data sources are used in an appropriate manner and can be applied to your study area to characterise drought for different time periods.

11.6 Further reading

Caretta, M.A., Mukherji, A., Arfanuzzaman, M., Betts, R.A., Gelfan, A., Hirabayashi, Y., Lissner, T.K., Liu, J., Lopez Gunn, E., Morgan, R., Mwanga, S., Supratid, S., 2022. Water, in: Pörtner, H.-O., Roberts, D.C., Tignor, M., Poloczanska, E.S., Mintenbeck, K., Alegría, A., Craig, M., Langsdorf, S., Löschke, S., Möller, V., Okem, A., Rama, B. (Eds.), Climate Change 2022: Impacts, Adaptation, and Vulnerability. Contribution of Working Group II to the Sixth Assessment Report of the Intergovernmental Panel on Climate Change, Cambridge University Press, Cambridge, UK and New York, NY, USA, pp. 379–550. https://doi.org/10.1017/9781009325844.005.

Cook, B.I., Mankin, J.S., Marvel, K., Williams, A.P., Smerdon, J.E., Anchukaitis, K.J., 2020. Twenty-first century drought projections in the CMIP6 forcing scenarios. Earth's Future 8(6), e2019EF001461. https://doi.org/10.1029/2019EF001461.

Ionita, M., Dima, M., Nagavciuc, V., Scholz, P., Lohmann, G., 2021. Past megadroughts in central Europe were longer, more severe and less warm than modern droughts. Commun. Earth Environ. 2, 61, https://doi.org/10.1038/s43247-021-00130-w.

Wada, Y., Bierkens, M.F.P., de Roo, A., Dirmeyer, P.A., Famiglietti, J.S., Hanasaki, N., Konar, M., Liu, J., Müller Schmied, H., Oki, T., Pokhrel, Y., Sivapalan, M., Troy, T. J., van Dijk, A.I.J.M., van Emmerik, T., Van Huijgevoort, M.H.J., Van Lanen, H.A.J., Vörösmarty, C.J., Wanders, N., Wheater, H., 2017. Human−water interface in hydrological modelling: current status and future directions. Hydrol. Earth Syst. Sci. 21, 4169-4193, https://doi.org/10.5194/hess-21-4169-2017.

References

Anchukaitis, K.J., 2017. Tree rings reveal climate change past, present, and future. Proc. Am. Philos Soc 161 (3), 244−263. https://www.jstor.org/stable/45211559.

Arnell, N.W., 2003. Effects of IPCC SRES* emissions scenarios on river runoff: a global perspective. Hydrol. Earth Syst. Sci. 7, 619−641. https://doi.org/10.5194/hess-7-619-2003.

Bakke, S.J., Ionita, M., Tallaksen, L.M., 2020. The 2018 northern European hydrological drought and its drivers in a historical perspective. Hydrol. Earth Syst. Sci. 24, 5621−5653. https://doi.org/10.5194/hess-24-5621-2020.

Barker, L.J., Hannaford, J., Parry, S., Smith, K.A., Tanguy, M., Prudhomme, C., 2019. Historic hydrological droughts 1891−2015: systematic characterisation for a diverse set of catchments across the UK. Hydrol. Earth Syst. Sci. 23, 4583−4602. https://doi.org/10.5194/hess-23-4583-2019.

Beven, K., Freer, J., 2001. Equifinality, data assimilation, and uncertainty estimation in mechanistic modelling of complex environmental systems using the GLUE methodology. J. Hydrol. 249 (1−4), 11−29. https://doi.org/10.1016/S0022-1694(01)00421-8.

Brunner, M.I., Slater, L., Tallaksen, L.M., Clark, M., 2020. Challenges in modeling and predicting floods and droughts: a review. Wires Wat. 8, e1520. https://doi.org/10.1002/wat2.1520.

Burek, P., Knijff, J.V.D., de Roo, A.D., 2013. LISFLOOD distributed water balance and flood simulation model. EU Joint Res. Center Tech. Rep. Ispra, Italy. https://doi.org/10.2788/24719.

Caillouet, L., Vidal, J.-P., Sauquet, E., Devers, A., Graff, B., 2017. Ensemble reconstruction of spatio-temporal extreme low-flow events in France since 1871. Hydrol. Earth Syst. Sci. 21, 2923−2951. https://doi.org/10.5194/hess-21-2923-2017.

Caillouet, L., Vidal, J.-P., Sauquet, E., Devers, A., Lauvernet, C., Graff, B., Vannier, O., 2021. Inter-comparison of extreme low-flow events in France since 1871. Hydrolog. Sci. J. 107 (1), 1−9. https://doi.org/10.1080/00186368.2021.1914463.

Caillouet, L., Vidal, J.-P., Sauquet, E., Graff, B., Soubeyroux, J.-M., 2019. SCOPE Climate: a 142-year daily high-resolution ensemble meteorological reconstruction dataset over France. Earth Syst. Sci. Data 11, 241–260. https://doi.org/10.5194/essd-11-241-2019.

Caretta, M.A., Mukherji, A., Arfanuzzaman, M., Betts, R.A., Gelfan, A., Hirabayashi, Y., Lissner, T.K., Liu, J., Lopez Gunn, E., Morgan, R., Mwanga, S., Supratid, S., 2022. Water. In: Pörtner, H.-O., Roberts, D.C., Tignor, M., Poloczanska, E.S., Mintenbeck, K., Alegría, A., Craig, M., Langsdorf, S., Löschke, S., Möller, V., Okem, A., Rama, B. (Eds.), Climate Change 2022: Impacts, Adaptation, and Vulnerability. Contribution of Working Group II to the Sixth Assessment Report of the Intergovernmental Panel on Climate Change. Cambridge University Press, Cambridge, UK and New York, NY, USA, pp. 379–550. https://doi.org/10.1017/9781009325844.005.

Compo, G.P., Whitaker, J.S., Sardeshmukh, P.D., Matsui, N., Allan, R.J., Yin, X., et al. 2011. The Twentieth century reanalysis project. Q. J. Roy Meteor. Soc. 137, 1–28. https://doi.org/10.1002/qj.776.

Cook, B.I., Mankin, J.S., Marvel, K., Williams, A.P., Smerdon, J.E., Anchukaitis, K.J., 2020. Twenty-first century drought projections in the CMIP6 forcing scenarios. Earth's Future 8 (6) e2019EF001461. https://doi.org/10.1029/2019EF001461.

Cook, B.I., Ault, T.R., Smerdon, J.E., 2015. Unprecedented 21st century drought risk in the American southwest and central plains. Sci. Adv. 1, e1400082. https://doi.org/10.1126/sciadv.1400082.

Corzo Perez, G.A., van Huijgevoort, M.H.J., Voss, F., Van Lanen, H.A.J., 2011. On the spatio-temporal analysis of hydrological droughts from global hydrological models. Hydrol. Earth Syst. Sci. 15, 2963–2978. https://doi.org/10.5194/hess-15-2963-2011.

Cucchi, M., Weedon, G.P., Amici, A., Bellouin, N., Lange, S., Müller Schmied, H., Hersbach, H., Buontempo, C., 2020. WFDE5: bias-adjusted ERA5 reanalysis data for impact studies. Earth Syst. Sci. Data 12, 2097–2120. https://doi.org/10.5194/essd-12-2097-2020.

Devers, A., Vidal, J.-P., Lauvernet, C., Vannier, O., 2021. FYRE Climate: a high-resolution reanalysis of daily precipitation and temperature in France from 1871 to 2012. Clim. Past 17, 1857–1879. https://doi.org/10.5194/cp-17-1857-2021.

Evans, N.P., Bauska, T.K., Gazquez-Sanchez, F., Brenner, M., Curtis, J.H., Hodell, D.A., 2018. Quantification of drought during the collapse of the classic Maya civilization. Science 361 (6401), 498–501. https://doi.org/10.1126/science.aas9871.

Forzieri, G., Feyen, L., Rojas, R., Flörke, M., Wimmer, F., Bianchi, A., 2014. Ensemble projections of future streamflow droughts in Europe. Hydrol. Earth Syst. Sci. 18, 85–108. https://doi.org/10.5194/hess-18-85-2014.

Garnier, E., 2019. Historic drought from archives: beyond the instrumental record. In: Iglesias, A., Assimacopoulos, D., Van Lanen, H.A.J. (Eds.), Drought: Science and Policy. Wiley Blackwell, John Wiley & Sons, Hoboken, USA, pp. 45–67. https://doi.org/10.1002/9781119017073.ch3.

Gernaat, D.E.H.J., Bogaart, P.W., van Vuuren, D.P., Biemans, H., Niessink, R., 2017. High-resolution assessment of global technical and economic hydropower potential. Nat. Energy 2, 821–828. https://doi.org/10.1038/s41560-017-0006-y.

Giuntoli, I., Villarini, G., Prudhomme, C., Mallakpour, I., Hannah, D.M., 2015. Evaluation of global impact models' ability to reproduce runoff characteristics over the central United States. J. Geophys. Res. Atmos. 120 (18), 9138–9159. https://doi.org/10.1002/2015JD023401.

Griffin, D., Anchukaitis, K.J., 2014. How unusual is the 2012–2014 California drought? Geophys. Res. Lett. 41, 9017–9023. https://doi.org/10.1002/2014GL062433.

Gudmundsson, L., Tallaksen, L.M., Stahl, K., Clark, D.B., Dumont, E., Hagemann, S., Bertrand, N., Gerten, D., Heinke, J., Hanasaki, N., Voss, F., Koirala, S., 2012. Comparing large-scale hydrological model simulations to observed runoff percentiles in Europe. J. Hydrometeorol. 13 (2), 604–620. https://doi.org/10.1175/JHM-D-11-083.1.

Gudmundsson, L., Leonard, M., Do, H.X., Westra, S., Seneviratne, S.I., 2019. Observed trends in global indicators of mean and extreme streamflow. Geophys. Res. Lett. 46, 756–766. https://doi.org/10.1029/2018GL079725.

Guo, D., Westra, S., Maier, H.R., 2017. Use of a scenario-neutral approach to identify the key hydro-meteorological attributes that impact runoff from a natural catchment. J. Hydrol. 554, 317–330. https://doi.org/10.1016/j.jhydrol.2017.09.021.

Guzha, A.C., Rufino, M.C., Okoth, S., Jacobs, S., Nóbrega, R.L.B., 2018. Impacts of land use and land cover change on surface runoff, discharge and low flows: evidence from East Africa. J. Hydrol Reg. Stud. 15, 49–67. https://doi.org/10.1016/j.ejrh.2017.11.005.

Haddeland, I., Clark, D.B., Franssen, W., Ludwig, F., Voss, F., Arnell, N.W., Bertrand, N., Best, M., Folwell, S., Gerten, D., Gomes, S., Gosling, S.N., Hagemann, S., Hanasaki, N., Harding, R., Heinke, J., Kabat, P., Koirala, S., Oki, T., Polcher, J., Stacke, T., Viterbo, P., Weedon, G.P., Yeh, P., 2011. Multi-model estimate of the global terrestrial water balance: setup and first results. J. Hydrometeorol. 12 (5), 869–884. https://doi.org/10.1175/2011JHM1324.1.

Haddeland, I., Heinke, J., Voß, F., Eisner, S., Chen, C., Hagemann, S., Ludwig, F., 2012. Effects of climate model radiation, humidity and wind estimates on hydrological simulations. Hydrol. Earth Syst. Sci. 16, 305–318. https://doi.org/10.5194/hess-16-305-2012.

Hannaford, J., Buys, G., Stahl, K., Tallaksen, L.M., 2013. The influence of decadal-scale variability on trends in long European streamflow records. Hydrol. Earth Syst. Sci. 17, 2717–2733. https://doi.org/10.5194/HESS-17-2717-2013.

Harding, R., Best, M., Blyth, E., Hagemann, S., Kabat, P., Tallaksen, L.M., Warnaars, T., Wiberg, D., Weedon, G.P., Van Lanen, H.A.J., Ludwig, F., Haddeland, I., 2011. Preface to the "water and global change (WATCH) special collection: current knowledge of the terrestrial global water cycle". J. Hydrometeorol. 12 (6), 1149–1156. https://doi.org/10.1175/JHM-D-11-024.1.

Hasan, H.H., Mohd Razali, S.F., Muhammad, N.S., Ahmad, A., 2019. Research trends of hydrological drought: a systematic review. Water 11, 2252. https://doi.org/10.3390/w11112252.

Ionita, M., Tallaksen, L.M., Kingston, D.G., Stagge, J.H., Laaha, G., Van Lanen, H.A.J., Scholz, P., Chelcea, S.M., Haslinger, K., 2017. The European 2015 drought from a climatological perspective. Hydrol. Earth Syst. Sci. 21, 1397–1419. https://doi.org/10.5194/hess-21-1397-2017.

Ionita, M., Dima, M., Nagavciuc, V., Scholz, P., Lohmann, G., 2021. Past megadroughts in central Europe were longer, more severe and less warm than modern droughts. Commun. Earth Environ. 2, 61. https://doi.org/10.1038/s43247-021-00130-w.

Laaha, G., Gauster, T., Tallaksen, L.M., Vidal, J.-P., Stahl, K., Prudhomme, C., Heudorfer, B., Vlnas, R., Ionita, M., Van Lanen, H.A.J., Adler, M.-J., Caillouet, L., Delus, C., Fendekova, M., Gailliez, S., Hannaford, J., Kingston, D., Van Loon, A.F., Mediero, L., Osuch, M., Romanowicz, R., Sauquet, E., Stagge, J.H., Wong, W.K., 2017. The European 2015 drought from a hydrological perspective. Hydrol. Earth Syst. Sci. 21, 3001–3024. https://doi.org/10.5194/hess-21-3001-2017.

Loaiciga, H.A., Haston, L., Michaelsen, J., 1993. Dendrohydrology and long-term hydrologic phenomena. Rev. Geophys. 31 (2), 151–171. https://doi.org/10.1029/93RG00056.

Možný, M., Brázdil, R., Dobrovolný, P., Trnka, M., Potopová, V., Hlavinka, P., Bartošová, L., Zahradníček, P., Štepánek, P., Žalud, Z., 2016. Drought reconstruction based on grape harvest dates for the Czech Lands, 1499–2012. Clim. Res. 70, 119–132. https://doi.org/10.3354/cr01423.

Maraun, D., Widmann, M., Gutiérrez, J.M., Kotlarski, S., Chandler, R.E., Hertig, E., Wibig, J., Huth, R., Wilcke, R.A.I., 2015. Value: a framework to validate downscaling approaches for climate change studies. Earth's Future 3, 1–14. https://doi.org/10.1002/2014EF000259.

Maraun, D., Widmann, M., 2018. Statistical Downscaling and Bias Correction for Climate Research. Cambridge University Press, Cambridge, UK.

Marx, A., Kumar, R., Thober, S., Zink, M., Wanders, N., Wood, E.F., Ming, P., Sheffield, J., Samaniego, L., 2018. Climate change alters low flows in Europe under a 1.5, 2, and 3 degree global warming. Hydrol. Earth Syst. Sci 22, 1017–1032. https://doi.org/10.5194/hess-22-1017-2018.

Meinshausen, M., Smith, S.J., Calvin, K., Daniel, J.S., Kainuma, M.L.T., Lamarque, J.F., Matsumoto, K., Montzka, S.A., Raper, S.C.B., Riahi, K., Thomson, A., Velders, G.J.M., Vuuren, D.P.P., 2011. The RCP greenhouse gas concentrations and their extensions from 1765 to 2300. Clim. Change 109, 213. https://doi.org/10.1007/s10584-011-0156-z.

Meko, D.M., Therrell, M.D., Baisan, C.H., Hughes, M.K., 2001. Sacramento river flow reconstructed to A.D. 869 from tree rings. J. Am. Water Resour. Assoc. 37, 1029−1039. https://doi.org/10.1111/j.1752-1688.2001.tb05530.x.

Melsen, L.A., Teuling, A.J., Torfs, P.J.J.F., Zappa, M., Mizukami, N., Mendoza, P.A., Clark, M.P., Uijlenhoet, R., 2019. Subjective modeling decisions can significantly impact the simulation of flood and drought events. J. Hydrol. 568, 1093−1104. https://doi.org/10.1016/j.jhydrol.2018.11.046.

Neukom, R., Luterbacher, J., Villalba, R., Küttel, M., Frank, D., Jones, P.D., Grosjean, M., Wanner, H., Aravena, J.-C., Black, D.E., Christie, D.A., D'Arrigo, R., Lara, A., Morales, M., Soliz-Gamboa, C., Srur, A., Urrutia, R., von Gunten, L., 2010a. Multiproxy summer and winter surface air temperature field reconstructions for southern South America covering the past centuries. Clim. Dynam. 37, 35−51. https://doi.org/10.1007/s00382-010-0793-3.

Neukom, R., Luterbacher, J., Villalba, R., Küttel, M., Frank, D., Jones, P.D., Grosjean, M., Esper, J., Lopez, L., Wanner, H., 2010b. Multi-centennial summer and winter precipitation variability in southern South America. Geophys. Res. Lett. 37, L14708. https://doi.org/10.1029/2010GL043680.

Pan, B., Anderson, G.J., Goncalves, A., Lucas, D.D., Bonfils, C.J.W., Lee, J., Tian, Y., Ma, H.-Y., 2021. Learning to correct climate projection biases. J. Adv. Model Earth Sys. 13. https://doi.org/10.1029/2021MS002509.

Prudhomme, C., Parry, S., Hannaford, J., Clark, D.B., Hagemann, S., Voss, F., 2011. How well do large-scale models reproduce regional hydrological extremes in Europe? J. Hydrometeorol. 12 (6), 1181−1204. https://doi.org/10.1175/2011JHM1387.1.

Prudhomme, C., Giuntoli, I., Robinson, E.L., Clark, D.B., Arnell, N.W., Dankers, R., Fekete, B.M., Franssen, W., Gerten, D., Gosling, S.N., Hagemann, S., Hannah, D.M., Kim, H., Masaki, Y., Satoh, Y., Stacke, T., Wada, Y., Wisser, D., 2014. Hydrological droughts in the 21st century. Proc. Natl. Acad. Sci. U.S.A 111 (9), 3262−3267. https://doi.org/10.1073/pnas.1222473110.

Riahi, K., van Vuuren, D.P., Kriegler, E., Edmonds, J., O'Neill, B.C., Fujimori, S., Bauer, N., Calvin, K., Dellink, R., Fricko, O., Lutz, W., Popp, A., Crespo Cuaresma, J., Samir, K.C., Leimbach, M., Jiang, L., Kram, T., Rao, S., Emmerling, J., Ebi, K., Hasegawa, T., Havlik, P., Humpenöder, F., Aleluia Da Silva, L., Smith, S., Stehfest, E., Bosetti, V., Eom, J., Gernaat, D., Masui, T., Rogelj, J., Strefler, J., Drouet, L., Krey, V., Luderer, G., Harmsen, M., Takahashi, K., Baumstark, L., Doelman, J.C., Kainuma, M., Klimont, Z., Marangoni, G., Lotze-Campen, H., Obersteiner, M., Tabeau, A., Tavoni, M., 2017. The shared socioeconomic pathways and their energy, land use, and greenhouse gas emissions implications: an overview. Glob. Environ. Change. 42, 153−168. https://doi.org/10.1016/j.gloenvcha.2016.05.009.

Sauchyn, D., Ilich, N., 2017. Nine hundred years of weekly streamflows: stochastic downscaling of ensemble tree-ring reconstructions. Water Resour. Res. 53, 9266−9283. https://doi.org/10.1002/2017WR021585.

Sauquet, E., Arama, Y., Blanc Coutagne, E., Bouscasse, H., Branger, F., Braud, I., Brun, J., Cherel, J., Cipriani, T., Datry, T., Ducharne, A., Hendrickx, F., Hingray, B., Krowicki, F., Le Goff, I., Le Lay, M., Magand, C., Malerbe, F., Mathevet, T., Monteil, C., Perrin, C., Poulhe, P., Rossi, A., Samie, R., Strosser, P., Thirel, G., Tilmant, F., Vidal, J.-P., 2016. Water allocation and uses in the Durance River basin in the 2050s: towards new management rules for the main reservoirs? Houille Blanche 102 (5), 25−31. https://doi.org/10.1051/lhb/2016046.

Sauquet, E., Shanafield, M., Hammond, J.C., Sefton, C., Leigh, C., Datry, T., 2021. Classification and trends in intermittent river flow regimes in Australia, northwestern Europe and USA: a global perspective. J. Hydrol. 597, 126170. https://doi.org/10.1016/j.jhydrol.2021.126170.

Smith, K.A., Barker, L.J., Tanguy, M., Parry, S., Harrigan, S., Legg, T.P., Prudhomme, C., Hannaford, J., 2019. A multi-objective ensemble approach to hydrological modelling in the UK: an application to historic drought reconstruction. Hydrol. Earth Syst. Sci. 23, 3247−3268. https://doi.org/10.5194/hess-23-3247-2019.

Smith, K.A., Tanguy, M., Hannaford, J., Prudhomme, C., 2018. Historic reconstructions of daily river flow for 303 UK catchments (1891−2015). NERC Environmental Information Data Centre, UK. https://data.gov.uk/dataset/0933be4b-fd96-4a7e-8de7-e2a37419a4ac/historic-reconstructions-of-daily-river-flow-for-303-uk-catchments-1891-2015.

Stagge, J.H., Rosenberg, D.E., DeRose, R.J., Rittenour, T.M., 2018. Monthly paleostreamflow reconstruction from annual tree-ring chronologies. J. Hydrol. 557, 791−804. https://doi.org/10.1016/j.jhydrol.2017.12.057.

Stahl, K., Hisdal, H., Hannaford, J., Tallaksen, L.M., Van Lanen, H.A.J., Sauquet, E., Demuth, S., Fendeková, M., Jódar, J., 2010. Streamflow trends in Europe: evidence from a dataset of near-natural catchments. Hydrol. Earth Syst. Sci. 14, 2376−2382. https://doi.org/10.5194/hess-14-2367-2010.

Stahl, K., Tallaksen, L.M., Hannaford, J., Van Lanen, H.A.J., 2012. Filling the white space on maps of European runoff trends: estimates from a multi-model ensemble. Hydrol. Earth Syst. Sci. 16, 2035−2047. https://doi.org/10.5194/hess-16-2035-2012.

Stahl, K., Tallaksen, L.M., Hannaford, J., 2019. Recent trends in historical drought. In: Iglesias, A., Assimacopoulos, D., Van Lanen, H.A.J. (Eds.), Drought: Science and Policy. Wiley Blackwell, John Wiley & Sons, Hoboken, USA, pp. 29−43. https://doi.org/10.1002/9781119017073.ch2.

Sutanto, S.J., Van Lanen, H.A.J., 2021. Streamflow drought: implication of drought definitions and its application for drought forecasting. Hydrol. Earth Syst. Sci. 25, 3991−4023. https://doi.org/10.5194/hess-25-3991-2021.

Sutanudjaja, E.H., van Beek, R., Wanders, N., Wada, Y., Bosmans, J.H.C., Drost, N., van der Ent, R.J., de Graaf, I.E.M., Hoch, J.M., de Jong, K., Karssenberg, D., López López, P., Peßenteiner, S., Schmitz, O., Straatsma, M.W., Vannametee, E., Wisser, D., Bierkens, M.F.P., 2018. PCR-GLOBWB 2: a 5 arcmin global hydrological and water resources model. Geosci. Model Dev. 11, 2429−2453. https://doi.org/10.5194/gmd-11-2429-2018.

Tallaksen, L.M., Stahl, K., 2014. Spatial and temporal patterns of large-scale droughts in Europe: model dispersion and performance. Geophys. Res. Lett. 41, 429−434. https://doi.org/10.1002/2013GL058573.

Tanguy, M., Prudhomme, C., Smith, K., Hannaford, J., 2018. Historical gridded reconstruction of potential evapotranspiration for the UK. Earth Syst. Sci. Data 10, 951−968. https://doi.org/10.5194/essd-10-951-2018.

Tingstand, A.H., Groves, D.G., Lempert, R.J., 2014. Paleoclimate scenarios to inform decision making in water resource management: example from Southern California's inland empire. J. Water Resour. Plan. Manag. 140 (10), 04014025. https://doi.org/10.1061/(ASCE)WR.1943-5452.0000403.

Torbenson, M.C.A., Stagge, J.H., 2021. Informing seasonal proxy-based flow reconstructions using baseflow separation: an example from the Potomac River, United States. Water Resour. Res. 57 (2), e2020WR027706. https://doi.org/10.1029/2020WR027706.

Van Huijgevoort, M.H.J., Hazenberg, P., Van Lanen, H.A.J., Teuling, R., Clark, D., Folwell, S., Gosling, S., Hanasaki, N., Heinke, J., Koirala, S., Stacke, T., Voβ, F., Sheffield, J., Uijlenhoet, R., 2013. Global multi-model analysis of hydrological drought in the second part of the 20th century (1963-2000). J. Hydrometeorol. 14, 1535−1552. https://doi.org/10.1175/JHM-D-12-0186.1.

Van Lanen, H.A.J., Laaha, G., Kingston, D.G., Gauster, T., Ionita, M., Vidal, J.-P., Vlnas, R., Tallaksen, L.M., Stahl, K., Hannaford, J., Delus, C., Fendekova, M., Mediero, L., Prudhomme, C., Rets, E., Romanowicz, R.J., Gailliez, S., Wong, W.K., Adler, M.-J., Blauhut, V., Caillouet, L., Chelcea, S., Frolova, N., Gudmundsson, L., Hanel, M., Haslinger, K., Kireeva, M., Osuch, M., Sauquet, E., Stagge, J.H., Van Loon, A.F., 2016. Hydrology needed to manage droughts: the 2015 European case. Hydrol. Process. 30, 3097−3104. https://doi.org/10.1002/hyp.10838.

Van Lanen, H.A.J., Prudhomme, C., Wanders, W., Van Huijgevoort, M.H.J., 2019. Future of drought. In: Iglesias, A., Assimacopoulos, D., Van Lanen, H.A.J. (Eds.), Drought: Science and Policy. Wiley Blackwell, John Wiley & Sons, Hoboken, USA, pp. 69–92. https://doi.org/10.1002/9781119017073.ch4.

Veldkamp, T.I.E., Zhao, F., Ward, P.J., De Moel, H., Aerts, J.C.J.H., Schmied, H.M., Portmann, F.T., Masaki, Y., Pokhrel, Y., Liu, X., Satoh, Y., Gerten, D., Gosling, S.N., Zaherpour, J., Wada, Y., 2018. Human impact parameterizations in global hydrological models improve estimates of monthly discharges and hydrological extremes: a multi-model validation study. Environ. Res. Lett. 13 (5), 055008. https://doi.org/10.1088/1748-9326/aab96f.

Vidal, J.-P., Hingray, B., Magand, C., Sauquet, E., Ducharne, A., 2016. Hierarchy of climate and hydrological uncertainties in transient low-flow projections. Hydrol. Earth Syst. Sci. 20, 3651–3672. https://doi.org/10.5194/hess-20-3651-2016.

Wada, Y., Bierkens, M.F.P., de Roo, A., Dirmeyer, P.A., Famiglietti, J.S., Hanasaki, N., Konar, M., Liu, J., Müller Schmied, H., Oki, T., Pokhrel, Y., Sivapalan, M., Troy, T.J., van Dijk, A.I.J.M., van Emmerik, T., Van Huijgevoort, M.H.J., Van Lanen, H.A.J., Vörösmarty, C.J., Wanders, N., Wheater, H., 2017. Human–water interface in hydrological modelling: current status and future directions. Hydrol. Earth Syst. Sci. 21, 4169–4193. https://doi.org/10.5194/hess-21-4169-2017.

Wanders, N., Wada, Y., 2015. Human and climate impacts on the 21st century hydrological drought. J. Hydrol. 527, 208–220. https://doi.org/10.1016/j.jhydrol.2014.10.047.

Wanders, N., Wada, Y., Van Lanen, H.A.J., 2015. Global hydrological droughts in the 21st century under a changing hydrological regime. Earth Syst. Dynam. 6, 1–15. https://doi.org/10.5194/esd-6-1-2015.

Warszawski, L., Frieler, K., Huber, V., Piontek, F., Serdeczny, O., Schewe, J., 2013. The inter-sectoral impact model Intercomparison project (ISI–MIP): project framework. Proc. Natl. Acad. Sci. U.S.A. 111, 3228–3232. https://doi.org/10.1073/pnas.1312330110.

Weedon, G.P., Gomes, S., Viterbo, P., Shuttleworth, W.J., Blyth, E., Österle, H., Adam, J.C., Bellouin, N., Boucher, O., Best, M., 2011. Creation of the WATCH forcing data and its use to assess global and regional reference crop evaporation over land during the Twentieth century. J. Hydrometeorol. 12 (5), 823–848. https://doi.org/10.1175/2011JHM1369.1.

Woodhouse, C.A., Lukas, J.J., 2006. Multi-century tree-ring reconstructions of Colorado streamflow for water resource planning. Clim. Change 78, 293–315. https://doi.org/10.1007/s10584-006-9055-0.

Woodhouse, C.A., Meko, D.M., MacDonald, G.M., Stahle, D.W., Cook, E.R., 2010. A 1,200-year perspective of 21st century drought in southwestern North America. Proc. Natl. Acad. Sci. U.S.A 107 (50), 21283–21288. https://doi.org/10.1073/pnas.0911197107.

Web references

URL 11.1 http://www.waterhistory.org/histories/cairo/cairo.pdf (Accessed March 25, 2022).
URL 11.2 https://esgf-node.llnl.gov/search/cmip6/ (Accessed February 1, 2022).